articles

molecular pharmaceutics

Mechanistic Modeling of Hepatic Transport from Cells to Whole Body: Application to Napsagatran and Fexofenadine

Agnès Poirier,*,† Christoph Funk,† Jean-Michel Scherrmann,‡ and Thierry Lavé†

Drug Safety, Non-Clinical Development, F. Hoffmann-La Roche Ltd., Basel, Switzerland, and Faculté de Pharmacie, Université Paris Descartes, INSERM U705, Paris, France

Received December 1, 2008; Revised Manuscript Received August 27, 2009; Accepted September 9, 2009

Abstract: A mechanistic model was applied to quantitatively derive the kinetic parameters from *in vitro* hepatic uptake transport data. These parameters were used as input to simulate *in vivo* elimination using a fully mechanistic physiologically based pharmacokinetic (PBPK) model. Fexofenadine and napsagatran, both BDDCS class 3 drugs, were chosen as model compounds. In rat, both compounds are hardly metabolized and are eliminated unchanged mostly through biliary excretion. Uptake was estimated in this study based on plated rat hepatocytes, and a mechanistic model was used to derive the active and passive transport parameters, namely Michaelis−Menten uptake parameters (V_{maxI} and $K_{mI,u}$) together with passive diffusion (P_{dif}) and nonspecific binding. Maximum transport velocity and passive diffusion were scaled to *in vivo* parameters (J_{maxI} and PS_{TC}) using hepatocellularity. Biliary excretion, through passive and active transport, was assessed from *in vivo* studies. These transport parameters were then used as input in a whole body physiologically based model in which the liver compartment was parametrized for the different passive and active transport processes. Each of the processes was linked to the free concentration in the relevant compartment. For napsagatran hepatic uptake, no passive diffusion and no binding were detected *in vitro* besides the active transport ($K_{mI,u}$ = 88.4 ± 8.1 μM, V_{maxI} = 384 ± 19 pmol/mg/min). Fexofenadine was rapidly taken up into rat hepatocytes ($K_{mI,u}$ = 271 ± 35 μM, V_{maxI} = 3162 ± 274 pmol/mg/min), and some contribution of passive diffusion to the uptake (P_{dif} = 2.08 ± 0.67 μL/mg/min) was observed. For fexofenadine, the biliary export rate was found to be slower than the uptake, leading to drug accumulation in liver. No accumulation was observed for napsagatran where excretion was faster than hepatic uptake. Observed plasma, liver and bile concentration time profiles were compared to PBPK simulations based on scaled *in vitro* transport kinetic parameters. An uncertainty analysis indicated that for both compounds the scaled *in vitro* uptake clearance had to be adjusted with an additional empirical scaling factor of 10 to match the plasma and liver concentrations and biliary excretion profiles. Applying this model, plasma clearance (CL_P) and half-life ($t_{1/2}$), maximum liver concentration (C_{maxL}) and fraction excreted in bile (f_{bile}) were predicted within 2-fold. *In vitro* uptake data had most impact on the simulated plasma and biliary excretion profiles, while accurate simulations of liver concentrations required also quantitative estimates of biliary excretion transport. This study indicated that the mechanistic model allowed for accurate evaluation of *in vitro* experiments; and the scaled kinetic parameters of hepatic uptake transport enabled the prediction of *in vivo* PK profiles and plasma clearances, using PBPK modeling.

Keywords: Transport; physiologically based pharmacokinetic (PBPK) modeling; liver; uptake; hepatocytes

 10.1021/mp8002495 CCC: $40.75
Published on Web 09/09/2009

Introduction

The disposition of compounds in the liver is influenced by many different factors such as metabolism, binding and transport. A number of studies have shown the possibility to successfully integrate *in vitro* metabolism data into physiologically based models in order to predict quantitatively *in vivo* profiles in animals and human.[1−3] Intrinsic metabolic clearance can be derived from depletion profiles of parent compound in hepatocyte and/or microsomal incubations. Physiologically based scaling can then be applied to scale the *in vitro* clearance to *in vivo* and account for nonspecific binding in the incubation medium, plasma protein binding and blood/plasma ratio.[4−8] This approach is mostly valid for highly permeable drugs (biopharmaceutics drug disposition classification system: BDDCS classes 1 and 2[9]) for which the impact of transporters on uptake is expected to be minimal. For low permeability compounds (BDDCS classes 3 and 4[9]), uptake and efflux transporters become critical determinants of the liver disposition.

The role of hepatic transporters in drug elimination as well as the current challenges for the *in vitro* evaluation and quantification of active and passive transport has been reviewed recently.[10−13] Dobson and Kell specifically assessed the importance of active drug uptake, underlying that the incorporation of active uptake processes into the rest of the metabolic network is an essential step for the prediction of human drug disposition.[14] The hepatic uptake of new chemical entities can be evaluated through *in vitro* experiments using hepatocytes or immortalized cell lines overexpressing specific transporters.[15] A mechanistic model to derive uptake parameters from hepatocytes and expressed cells was recently described by Poirier et al.[16] In this study, a mechanistic model was proposed which describes two compartments, the *in vitro* uptake assay for the quantification of nonspecific binding, bidirectional passive diffusion, and active uptake processes. The proposed mechanistic model led to significant improvements over the conventional two-step approach (where in a first step initial uptake rates are determined to be plotted against substrate concentrations in a second step) for the estimation of transport parameters.[16]

A mechanistic liver PBPK model must allow for discrimination of distinct kinetic processes, i.e. uptake by passive and active transport, distribution, metabolism (e.g., P450 oxidation and conjugation) and excretion (biliary excretion). Parameters for each of the above processes must be obtained from physicochemical properties and from *in vitro* data and must then be linked to the appropriate drug concentration within the relevant medium (i.e., free concentration in plasma for the uptake processes, and the intracellular free drug concentration for the efflux, metabolism and excretion processes). Quantitative predictions of *in vivo* pharmacokinetic profiles of actively transported drugs have been attempted only in a few studies. Recently, Paine et al.[17]

* Corresponding author: F. Hoffmann-La Roche Ltd., Drug Metabolism and Pharmacokinetics, PRNBDDM1, Bldg 69/103, CH-4070 Basel, Switzerland. E-mail: agnes.poirier@roche.com. Tel: +41 (0)61 68 72904. Fax: +41 61 688 2908.

† F. Hoffmann-La Roche Ltd.

‡ Université Paris Descartes.

(1) Parrott, N.; Jones, H.; Paquereau, N.; Lave, T. Application of full physiological models for pharmaceutical drug candidate selection and extrapolation of pharmacokinetics to man. *Basic Clin. Pharmacol. Toxicol.* **2005**, *96*, 193–9.

(2) Rostami-Hodjegan, A.; Tucker, G. T. Simulation and prediction of in vivo drug metabolism in human populations from in vitro data. *Nat. Rev. Drug Discovery* **2007**, *6*, 140–8.

(3) Jones, H. M.; Parrott, N.; Jorga, K.; Lave, T. A novel strategy for physiologically based predictions of human pharmacokinetics. *Clin. Pharmacokinet.* **2006**, *45*, 511–42.

(4) Ito, K.; Houston, J. B. Prediction of human drug clearance from in vitro and preclinical data using physiologically based and empirical approaches. *Pharm. Res.* **2005**, *22*, 103–12.

(5) Soars, M. G.; Grime, K.; Sproston, J. L.; Webborn, P. J.; Riley, R. J. Use of hepatocytes to assess the contribution of hepatic uptake to clearance in vivo. *Drug Metab. Dispos.* **2007**, *35*, 859–65.

(6) Ito, K.; Houston, J. B. Comparison of the use of liver models for predicting drug clearance using in vitro kinetic data from hepatic microsomes and isolated hepatocytes. *Pharm. Res.* **2004**, *21*, 785–92.

(7) Riley, R. J.; McGinnity, D. F.; Austin, R. P. A unified model for predicting human hepatic, metabolic clearance from in vitro intrinsic clearance data in hepatocytes and microsomes. *Drug Metab. Dispos.* **2005**, *33*, 1304–11.

(8) McGinnity, D. F.; Soars, M. G.; Urbanowicz, R. A.; Riley, R. J. Evaluation of fresh and cryopreserved hepatocytes as in vitro drug metabolism tools for the prediction of metabolic clearance. *Drug Metab. Dispos.* **2004**, *32*, 1247–53.

(9) Wu, C. Y.; Benet, L. Z. Predicting drug disposition via application of BCS: transport/absorption/elimination interplay and development of a biopharmaceutics drug disposition classification system. *Pharm. Res.* **2005**, *22*, 11–23.

(10) Funk, C. The role of hepatic transporters in drug elimination. *Expert Opin. Drug Metab. Toxicol.* **2008**, *4*, 363–79.

(11) Mizuno, N.; Niwa, T.; Yotsumoto, Y.; Sugiyama, Y. Impact of drug transporter studies on drug discovery and development. *Pharmacol. Rev.* **2003**, *55*, 425–61.

(12) Shitara, Y.; Horie, T.; Sugiyama, Y. Transporters as a determinant of drug clearance and tissue distribution. *Eur. J. Pharm. Sci.* **2006**, *27*, 425–46.

(13) Endres, C. J.; Hsiao, P.; Chung, F. S.; Unadkat, J. D. The role of transporters in drug interactions. *Eur. J. Pharm. Sci.* **2006**, *27*, 501–17.

(14) Dobson, P. D.; Kell, D. B. Carrier-mediated cellular uptake of pharmaceutical drugs: an exception or the rule. *Nat. Rev. Drug Discovery* **2008**, *7*, 205–20.

(15) Poirier, A.; Funk, C.; Lave, T.; Noe, J. New strategies to address drug-drug interactions involving OATPs. *Curr. Opin. Drug Discovery Dev.* **2007**, *10*, 74–83.

(16) Poirier, A.; Lave, T.; Portmann, R.; Brun, M. E.; Senner, F.; Kansy, M.; Grimm, H. P.; Funk, C. Design, data analysis and simulation of in vitro drug transport kinetic experiments using a mechanistic in vitro model. *Drug Metab. Dispos.* **2008**, *36*, 2434–44.

(17) Paine, S. W.; Parker, A. J.; Gardiner, P.; Webborn, P. J. H.; Riley, R. J. Prediction of the Pharmacokinetics of Atorvastatin, Cerivastatin and Indomethacin Using Kinetic Models Applied to Isolated Rat Hepatocytes. *Drug Metab. Dispos.* **2008**, *36* (7), 1365–74.

showed successful predictions of the pharmacokinetics of atorvastatin, cerivastatin and indomethacin using uptake data from isolated rat hepatocytes combined with a semiphysiologically based modeling approach. Most of the modeling studies dealing with hepatobiliary transported drugs are based on optimized compartmental models. In this context, there have been a number of attempts to model the liver as one or more compartments.[18−20] Using a PBPK model, Ploeger et al. were able to simulate the glycyrrhizic acid pharmacokinetics by integration of Michaelis−Menten parameters fitted from *in vivo* data.[21] This is of limited interest in a drug discovery context where the prediction of liver kinetics needs to be based on *in vitro* and/or *in silico* data.

In order to develop and validate a methodology for *in vivo* prediction of PK profiles for compounds actively taken up into the liver based on *in vitro* uptake data and physiologically based models, we have selected two BDDCS class 3 compounds for which transporter effects predominate.[9] Fexofenadine and napsagatran are metabolically stable, and their hepatic elimination is mainly driven by active transport. Napsagatran is a low molecular weight thrombin inhibitor eliminated unchanged in urine and bile.[22] While the transport proteins responsible for napsagatran transport are still unknown, selective accumulation in liver and kidney tissues suggested significant involvement of active transport. Fexofenadine, a nonsedating antihistamine drug, is the active metabolite of terfenadine and is widely used as a model substrate to study active transport.[23−26] In rats, fexofenadine has been described to be eliminated unchanged in urine and bile and it was found to be a substrate of Oatp1a1 and 1a4 (hepatic uptake), Mrp3 (hepatic efflux), Mdr1 and Abcc11 (biliary excretion).[24,26]

The aim of this study was to evaluate the relevance of uptake parameters obtained in hepatocyte incubations for the prediction of *in vivo* pharmacokinetic parameters and concentration time profiles in plasma, bile and liver. Thus, the disposition of napsagatran and fexofenadine has been studied and evaluated using a physiologically based model that addresses processes such as binding, uptake, permeability, distribution and elimination.

Materials and Methods

Materials. [^{3}H]-Fexofenadine (racemic mixture) was obtained from Moravek Biochemicals (Brea, CA). Fexofenadine (racemic mixture) was from Sigma (Buchs, Switzerland). Napsagatran and [^{14}C]-napsagatran were synthesized in-house. All cell culture media and reagents were purchased from Invitrogen Corporation (Paisley, U.K.), and standard tissue culture flasks and 24-well plates were from Falcon/Becton Dickinson (Franklin Lakes, NJ).

Preparation and Plating of Primary Rat Hepatocytes. Isolation and conventional primary culture of rat hepatocytes were performed as described previously.[27,28] Hepatocytes were isolated from adult male Wistar rat (∼250 g) livers by a previously described two-step collagenase perfusion method.[27,29] Cell viability was determined from exclusion of erythrosine-B by the cell membranes. Only the cell preparations that exhibited a viability over 80% were used in further studies. Freshly prepared hepatocytes were seeded at 4×10^5 cells/well on precoated 24-well plates (Becton Dickinson BioCoat Collagen I). Cells were cultured for 3 h in a humidified atmosphere maintained at 37 °C, 5% CO_2 in attachment medium composed of Williams' E medium supplemented with 10% fetal calf serum, 0.5% streptomycin/penicillin, insulin (1.2 μM) and glutamine (400 μM).

***In Vitro* Uptake Experiments.** Rat hepatocytes were prepared as outlined above, and the uptake assays were performed as described previously.[16] Assays were run using two wells as one set. The medium was removed from the wells by aspiration. The wells were washed once with 1 mL

(18) Hatanaka, T.; Honda, S.; Sasaki, S.; Katayama, K.; Koizumi, T. Pharmacokinetic and pharmacodynamic evaluation for tissue-selective inhibition of cholesterol synthesis by pravastatin. *J. Pharmacokinet. Biopharm.* **1998**, *26*, 329–47.

(19) Andersen, M. E.; Eklund, C. R.; Mills, J. J.; Barton, H. A.; Birnbaum, L. S. A multicompartment geometric model of the liver in relation to regional induction of cytochrome P450s. *Toxicol. Appl. Pharmacol.* **1997**, *144*, 135–44.

(20) Deroubaix, X.; Coche, T.; Depiereux, E.; Feytmans, E. Saturation of hepatic transport of taurocholate in rats in vivo. *Am. J. Physiol.* **1991**, *260*, G189–96.

(21) Ploeger, B.; Mensinga, T.; Sips, A.; Seinen, W.; Meulenbelt, J.; DeJongh, J. The pharmacokinetics of glycyrrhizic acid evaluated by physiologically based pharmacokinetic modeling. *Drug Metab. Rev.* **2001**, *33*, 125–47.

(22) Lave, T.; Portmann, R.; Schenker, G.; Gianni, A.; Guenzi, A.; Girometta, M. A.; Schmitt, M. Interspecies pharmacokinetic comparisons and allometric scaling of napsagatran, a low molecular weight thrombin inhibitor. *J. Pharm. Pharmacol.* **1999**, *51*, 85–91.

(23) Matsushima, S.; Maeda, K.; Ishiguro, N.; Igarashi, T.; Sugiyama, Y. Investigation of the inhibitory effects of various drugs on the hepatic uptake of fexofenadine in humans. *Drug Metab. Dispos.* **2008**, *36* (4), 663–9.

(24) Matsushima, S.; Maeda, K.; Hayashi, H.; Debori, Y.; Schinkel, A. H.; Schuetz, J. D.; Kusuhara, H.; Sugiyama, Y. Involvement of multiple efflux transporters in hepatic disposition of fexofenadine. *Mol. Pharmacol.* **2008**, *73* (5), 1474–83.

(25) Kamath, A. V.; Yao, M.; Zhang, Y.; Chong, S. Effect of fruit juices on the oral bioavailability of fexofenadine in rats. *J. Pharm. Sci.* **2005**, *94*, 233–9.

(26) Cvetkovic, M.; Leake, B.; Fromm, M. F.; Wilkinson, G. R.; Kim, R. B. OATP and P-glycoprotein transporters mediate the cellular uptake and excretion of fexofenadine. *Drug Metab. Dispos.* **1999**, *27*, 866–71.

(27) Luttringer, O.; Theil, F. P.; Lave, T.; Wernli-Kuratli, K.; Guentert, T. W.; de Saizieu, A. Influence of isolation procedure, extracellular matrix and dexamethasone on the regulation of membrane transporters gene expression in rat hepatocytes. *Biochem. Pharmacol.* **2002**, *64*, 1637–50.

(28) Blanchard, N.; Richert, L.; Notter, B.; Delobel, F.; David, P.; Coassolo, P.; Lave, T. Impact of serum on clearance predictions obtained from suspensions and primary cultures of rat hepatocytes. *Eur. J. Pharm. Sci.* **2004**, *23*, 189–99.

(29) Seglen, P. O. Hepatocyte suspensions and cultures as tools in experimental carcinogenesis. *J. Toxicol. Environ. Health* **1979**, *5*, 551–60.

of HBSS (Hanks balanced salt solution (InVitrogen/GIBCO) containing calcium and magnesium) at 37 °C. The uptake experiments were started by aspiration of wash buffer and adding 150 μL of a prewarmed 37 °C HBSS solution containing the substrate of interest. The plates were incubated on a 37 °C heating block (Eppendorf), and after the indicated times the uptake was stopped immediately by addition of 1 mL of ice-cold PBS containing 0.2% bovine serum albumin (BSA) and removal of the solution by aspiration. BSA was also included in the subsequent washing buffer to minimize background due to nonspecific binding of radiolabeled compound. The following washing steps were performed rapidly with warmed (37 °C) buffer. The cells were washed twice with 2 mL of PBS each, containing 0.2% BSA and once with PBS without BSA (3 mL) to remove added BSA protein. Then 0.5 mL of 1% TritonX was added to solubilize the cells. After incubation for 15 min on a heated shaker at 60 °C, 0.25 mL of the solubilized cell mix was added to 4 mL of scintillation fluid and radioactivity was determined by liquid scintillation counting. The total protein content was determined for each well using the Pierce BCA assay (Pierce, Rockford, IL) with BSA as standard according to the manufacturers' protocol.

Kinetic *in Vitro* Experiment. Kinetic experiments were carried out as described above on 24-well plates. One experiment consisted of the drug of interest incubated at 7 or 8 different concentrations which were adjusted after a first experiment to allow for proper K_m and P_{dif} evaluation. Three different time points were used per drug concentration (30 s, 60 s and 90 s), and each time point was done in duplicate. Kinetic parameters were calculated using the whole data set in a single step as described later. Three independent experiments using different batches of fresh hepatocytes, prepared from a different rat each, were made for calculation of mean kinetic parameters.

***In Vivo* Studies.** All *in vivo* studies were conducted in accordance with local regulations for animal treatment. Male Wistar rats (7−8 weeks, 0.283 ± 0.034 kg) were purchased from Charles River (Germany) and were used in the *in vivo* studies with fexofenadine. Albino rats (SPF RoRo, 6−7 weeks, 0.240 ± 0.010 kg) were obtained from BRL (Füllinsdorf, Switzerland) and used in the *in vivo* studies with napsagatran. Animals were kept under standard laboratory conditions on a 12 h light/dark cycle in controlled conditions (22 °C, 55% humidity) with continuous access to dry pellet food and tap water. They were acclimatized for a minimum of 1 day before experiments were performed.

Plasma Concentration Time Profiles. At least one day before administration of the test compound, operations on animals were performed after treatment with 0.05 mg/kg buprenorphin sc and anesthesia with ketamine and xylamine. A catheter was implanted into the jugular vein.

For the intravenous administration (bolus), the solution containing test compound (∼1 mL/kg) was injected through the jugular vein catheter. Following the injection, the catheter was washed twice by aspiration and reinjection of approximately 0.2−0.3 mL of blood followed by injection of 0.5 mL of physiologic saline solution.

Napsagatran was formulated in 1:4 (v/v) DMSO/distilled water. The concentration of the solution was approximately 10 mg/mL and was injected at a constant rate (∼1 mL/h) over 90 min. Fexofenadine (unlabeled) was dissolved in 30% (v/v) 1-methyl-2-pyrrolidone and 70% (v/v) NaCl 0.9%, and this solution was used for iv bolus administration or intravenous infusion at a constant rate (∼1 mL/h) over 30 min.

At designated time points (5, 10, 20, 30, 40, 50, 60, 80, and 100 min for napsagatran and 5, 15, 30 min, 1, 2, 4, 8, and 24 h for fexofenadine), 0.3 mL blood samples were collected with a 1 mL syringe from the catheter implanted into the jugular vein, gently mixed and then transferred to microcentrifuge tubes containing EDTA and sodium fluoride as anticoagulant and stabilizer. To maintain the blood volume, the corresponding volume of physiologic saline solution was injected after the collection of each blood sample. Blood samples during the infusion time were taken sublingually under anesthesia. All blood samples were immediately centrifuged at 3000*g* for 5 min at a temperature of 4 °C. The plasma was transferred into microcentrifuge tubes and stored frozen at −20 °C until analysis.

Urine samples from rats housed individually in metabolic cages were collected on ice in fractions (0−3 h and 3−6 h for napsagatran, 0−8 h and 8−24 h for fexofenadine).

Liver Concentration Time Profiles. Fexofenadine was administered as described for the plasma infusion study. The anesthetized animals were sacrificed at 0.5, 1, 2, and 4 h by heart puncture (plasma sampled), and the liver was collected, blotted dry with absorbent paper without washing, weighed and stored frozen at −20 °C until preparation and analysis.

[^{14}C]-Napsagatran was administered intravenously (bolus, 2.19 MBq/kg) via the tail vein of the conscious animals. For administration, 5 mg of [^{14}C]-napsagatran and 9 mg of sodium chloride were dissolved in 0.4 mL of 0.2 M lactic acid solution; the final volume was adjusted to 1 mL using distilled water. The animals were sacrificed under anesthesia at 5, 20 min, 1 and 24 h, by exsanguination and the liver was collected, blotted dry with absorbent paper without washing and weighed. The tissue was dissolved with NaOH (5 N at 50 °C for 36 h) before liquid scintillation counting.

Biliary Excretion-Time Profiles. The rats dosed with fexofenadine were anesthetized with 90 mg/kg ketamine and 10 mg/kg xylazine. Two catheters were implanted into the jugular vein and the bile duct, respectively. Directly after the operation, compounds were administered by the jugular vein (same schedule described as for the plasma concentration profile). Bile samples were collected in 20 min fractions at room temperature, and liver was collected as described above, at the end of the experiment. The rats were under anesthesia for the whole experiment (operation and sampling, about 4 h).

To study the biliary excretion of napsagatran, three catheters were implanted, one in the jugular vein and two in

the bile duct, under anesthesia with pentobarbital. Compounds were administered and plasma was collected as described for the plasma concentration time profile studies. The animals were conscious during administration and sampling. Bile samples from rats were collected on ice in 30 min fractions over 2 h.

Sample Analysis. All samples were stored frozen at −20 °C until analysis.

Plasma concentrations of fexofenadine were determined using reversed-phase HPLC with triple quadrupole tandem mass spectrometry (MS/MS) detection. Briefly, plasma samples were deproteinized with acetonitrile containing the internal standard (midazolam-d_6). After dilution of the supernatant, the samples were analyzed on a reversed-phase column and quantified by multiple reaction monitoring (MRM m/z 332→297 for fexofenadine; MRM m/z 295→267 for internal standard) in positive ionization mode on an AB-SCIEX API3000 triple quadrupole mass spectrometer using turbo ion spray ionization. The lower limit of quantification of the assay was 5 ng/mL. An aliquot of each liver sample (approximately 1 g) was homogenized by ultrasonication with 4 aliquots of water. For analysis, the bile and urine samples were diluted with rat blank plasma (respectively 1/100 and 1/25) and the liver homogenates were diluted with blank liver homogenates (1/5). Bile, urine and liver homogenates were analyzed utilizing the method described for the analysis of plasma samples.

Napsagatran concentrations in plasma, bile and urine from the different studies were determined by reversed phase HPLC-UV. Briefly, plasma samples were deproteinized with acetonitrile and, after evaporation and reconstitution of the supernatant, the samples were analyzed by reversed-phase HPLC using a C_{18} column (Supelcosil LC 18-DB, 5 μm 150 × 4.6 mm) and UV detection at 234 nm. Bile and urine samples were diluted (1:60) with the mobile phase (20 mM KH_2 PO_4/acetonitrile 750/250) prior to analysis. The limit of quantification of the assay was 50 ng/mL for plasma and 5 μg/mL for urine and bile. The liver [^{14}C]-napsagatran levels were measured using liquid scintillation counting after homogenization.

Data Analysis of *In Vitro* Uptake Experiments Using Compartmental Model. The cellular uptake process consists of both an active, saturable process and a passive component. The active transport can be characterized by Michaelis−Menten parameters (V_{maxI}, $K_{mI,u}$), while the passive process is represented by the passive diffusion P_{dif}. A mechanistic two-compartment model was used to determine those three parameters from the *in vitro* uptake experiment, as described previously.[16]

The *in vitro* assay was described by two compartments corresponding to the incubation medium for one well (150 μL, volume V_{ex} and compound concentration C_{ex} in μM) and the intracellular space of all cells in one well (volume V_{int}, quantity of compound in one well A_{int} in pmol and compound concentration in μM $C_{int} = A_{int}/V_{int}$). For the determination of V_{int} (in μL), the total quantity of protein per well (U_{int} in mg) was converted to number of cells by applying an experimentally determined constant of 1 mg total protein per million rat hepatocytes (MTPMH = 1.06 ± 0.18 mg/10^{6}cells, n = 5, similar to a reported value[30]). A cell volume of 3.9 μL per million hepatocytes[31] was then applied to calculate the intracellular volume in μL in one well: $V_{int} = (U_{int}/\text{MTPMH}) \times 3.9$ (the mean observed value for V_{int} was 0.90 ± 0.09 μL ranging from 0.72 to 1.14 μL).

The time-course of the quantity of compound in the intracellular compartment was modeled by the following differential equation:

$$V_{int}\frac{dC_{int}}{dt} = \frac{V_{maxI} \times C_{ex}}{K_{mI,u} + C_{ex}} + P_{dif}(C_{ex} - C_{int}) \qquad (1.1)$$

In eq 1.1, V_{maxI} was expressed in pmol/min, $K_{mI,u}$ in μM, and P_{dif} in μL/min and all three calculated parameters were calculated relative to the cells in one well. P_{dif} and V_{maxI} were corrected for the total amount of protein in one well ($U_{intracell}$ in mg).[16] A nonzero initial condition for the intracellular compound was used to account for nonspecific binding to cells and/or experimental supports (f_b). This amount was assumed to be proportional to C_{ex} and V_{int} and f_b, the bound fraction:

$$A_{int}(t = 0) = f_b \times C_{ex} \times V_{int} \qquad (1.2)$$

This mechanistic *in vitro* model was implemented in ModelMaker v.4 (AP Benson, U.K.). Numerical integration was performed using the Runge−Kutta fourth order method. The Marquardt optimization algorithm (weighted least-squares) was used to simultaneously estimate the parameters f_b, V_{maxI}, P_{dif} and $K_{mI,u}$.

Pharmacokinetic Analysis. Plasma concentration time data for observed and simulated profiles were analyzed by noncompartmental methods using the PKPlus module of GastroPlus. The slope of the terminal phase, β, was determined by log-linear regression of the last two or three data points, and the terminal half-life was calculated as $t_{1/2} = 0.693/\beta$. The area under the plasma concentration time curve (AUC_∞^0) and area under the moment curve ($AUMC_\infty^0$) were calculated by use of the linear trapezoidal rule, and log extrapolation to time infinity by adding C/β to AUC_{last}^0 and $tC/\beta + C/\beta^2$ to $AUMC_{last}^0$, where C is the last predicted concentration at the last sampling time t. The plasma systemic clearance (CL_P) was calculated by use of the relationship CL_P = dose/AUC_∞^0. The volume of distribution at steady state (Vd_{SS}) was calculated from $Vd_{SS} = CL_P \times (AUMC_\infty^0/AUC_\infty^0)$ for intravenous bolus administration and $Vd_{SS} = CL_P \times [(AUMC_\infty^0/AUC_\infty^0) - (\tau/2)]$, where τ is the infusion time, for intravenous infusion.

(30) Shitara, Y.; Hirano, M.; Adachi, Y.; Itoh, T.; Sato, H.; Sugiyama, Y. In vitro and in vivo correlation of the inhibitory effect of cyclosporin A on the transporter-mediated hepatic uptake of cerivastatin in rats. *Drug Metab. Dispos.* **2004**, *32*, 1468–75.

(31) Reinoso, R. F.; Telfer, B. A.; Brennan, B. S.; Rowland, M. Uptake of teicoplanin by isolated rat hepatocytes: comparison with in vivo hepatic distribution. *Drug Metab. Dispos.* **2001**, *29*, 453–9.

For both compounds, the liver concentrations were corrected for residual blood and bile in the collected liver using published values for blood and bile within the liver tissue of 25.2%[32] and 0.43%[33] of the liver volume, respectively. The quantity of remaining compound in blood and bile at the time of the liver collection was calculated based on plasma and bile concentration time profiles and subtracted from the total compound measured in liver tissue.

The fraction of the dose excreted unchanged in bile (f_{bile}) was calculated as the ratio of the total quantity in bile over the nominal dose administered.

The fraction of the dose excreted unchanged in urine (fe) was calculated as the ratio of the total quantity in urine over the nominal dose administered. The fraction fe was then used to calculate the observed *in vivo* plasmatic renal clearance (CL_{RP}) as follows: $CL_{RP} = CL_P \times fe$.

Biliary Excretion Rate Calculation. The clearance corresponding to the excretion of the unchanged compound from the liver tissue into bile through active and passive processes was obtained from *in vivo* data. For this purpose the biliary excretion rates were correlated to the total liver concentrations and $K_{mE,u}$, J_{maxE} and PS_{TCAp} were fitted using eq 2.1:

$$\frac{\Delta M_{bile}}{\Delta t} = \frac{J_{maxE} \times C_L \times fu_L}{C_L \times fu_L + K_{mE,u}} + PS_{TCAp} \times C_L \times fu_L \quad (2.1)$$

In this equation, C_L is the total concentration in liver corrected for residual biliary and blood concentrations, M_{bile} the amount of drug cleared by biliary excretion during bile collection time intervals (Δt) and PS_{TCAp} the permeability−surface area product for the apical membrane. The passive permeability was considered unidirectional assuming therefore that compound diffusion occurs only from hepatocytes into bile. The liver unbound fraction fu_L was calculated according to Rodgers and Rowland[34,35] as described in eqs 3.1 and 3.2. $K_{mE,u}$, J_{maxE} and PS_{TCAp} were defined as lumped values and were obtained by fitting the biliary excretion rate as a function of liver concentration corrected for blood and bile content using XLfit 4.1.1 (ID Business Solutions, Guildford, U.K.).

Whole Body PBPK Model. A whole body PBPK model for rat was used in this study. The model included 14 tissue compartments (adipose, red bone marrow, yellow bone marrow, brain, gut, heart, kidney, liver, lung, muscle, reproductive organs, rest of body, skin, and spleen) linked by the blood circulation. An overview of whole body PBPK models including equations for flow and diffusion limited distribution is given in Nestorov (2007) and Rowland et al. (2004).[36,37] The physiological parameters such as tissue volumes, blood flow and tissue compositions (lipids and water) published in Poulin and Theil (2002)[38,39] were used in this study.

For both compounds, permeability limited distribution was assumed only for the liver compartment which was parametrized accordingly to integrate the permeability data measured in hepatocytes. Such an assumption would be fully justified for the other distribution organs as well, especially in light of the concave shape of the plasma concentration profile which suggests a long lasting distribution and redistribution processes driven by permeation challenges. However, no permeability data was available for the other tissues, therefore perfusion limited distribution was assumed.

For both compounds, liver and kidney were assumed to be the eliminating organs. The mathematical model was available in the simulation software GastroPlus 6.0.0 (Simulations Plus Inc., CA).

The input data for both compounds were the molecular weights, logD, pK_a and fu_P values, the blood−plasma ratios (R_{bp}), renal clearances, animal weights and doses. As described in Figure 1, the simulated plasma, liver and bile profiles were analyzed by noncompartmental analysis (as described in previous sections) to derive CL_P, $t_{1/2}$, maximum liver concentration (C_{maxL}) and fraction excreted in bile (f_{bile}) for comparison to the *in vivo* observations.

1. *K*p and fu_T Calculations. The calculation of unbound fraction in intracellular space fu_T was based on tissue composition models according to Rodgers et al.[34,35] The different equations used for fu_T in perfusion and permeability-limited tissues were derived from the work of Lukacova et al.[41] and are described below; the abbreviations used are detailed in the abbreviations section.

For perfusion-limited tissues (eq 3.1), the basic assumptions are as follows:

(32) Khor, S. P.; Bozigian, H.; Mayersohn, M. Potential error in the measurement of tissue to blood distribution coefficients in physiological pharmacokinetic modeling. Residual tissue blood. II. Distribution of phencyclidine in the rat. *Drug Metab. Dispos.* **1991**, *19*, 486–90.

(33) Blouin, A.; Bolender, R. P.; Weibel, E. R. Distribution of organelles and membranes between hepatocytes and nonhepatocytes in the rat liver parenchyma. A stereological study. *J. Cell Biol.* **1977**, *72*, 441–55.

(34) Rodgers, T.; Rowland, M. Physiologically based pharmacokinetic modelling 2: predicting the tissue distribution of acids, very weak bases, neutrals and zwitterions. *J. Pharm. Sci.* **2006**, *95*, 1238–57.

(35) Rodgers, T.; Leahy, D.; Rowland, M. Physiologically based pharmacokinetic modeling 1: predicting the tissue distribution of moderate-to-strong bases. *J. Pharm. Sci.* **2005**, *94*, 1259–76.

(36) Nestorov, I. Whole-body physiologically based pharmacokinetic models. *Expert Opin. Drug Metab. Toxicol.* **2007**, *3*, 235–49.

(37) Rowland, M.; Balant, L.; Peck, C. Physiologically based pharmacokinetics in Drug Development and Regulatory Science: A workshop report (Georgetown University, Washington, DC, May 29−30, 2002. *AAPS J.* **2004**, *6*, 56–67.

(38) Poulin, P.; Theil, F. P. Prediction of pharmacokinetics prior to in vivo studies. 1. Mechanism-based prediction of volume of distribution. *J. Pharm. Sci.* **2002**, *91*, 129–56.

(39) Poulin, P.; Theil, F. P. Prediction of pharmacokinetics prior to in vivo studies. II. Generic physiologically based pharmacokinetic models of drug disposition. *J. Pharm. Sci.* **2002**, *91*, 1358–70.

(40) Parrott, N.; Paquereau, N.; Coassolo, P.; Lave, T. An evaluation of the utility of physiologically based models of pharmacokinetics in early drug discovery. *J. Pharm. Sci.* **2005**, *94*, 2327–43.

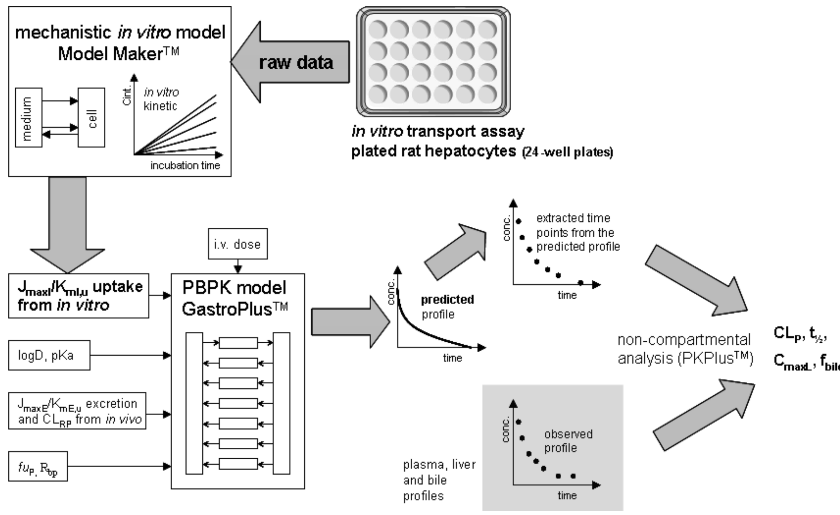

Figure 1. Steps taken in the evaluation (adapted from ref 40).

(a) well stirred compartment, instant equilibrium between the extracellular and intracellular concentrations;
(b) unbound, nonionized compound concentrations in extracellular, intracellular, and plasma regions are equal.

$$\mathrm{fu_T} = [2 + 10^{(\mathrm{p}K\mathrm{aBase}-\mathrm{pH_{EW}})} + 10^{(\mathrm{p}K\mathrm{aBase}-\mathrm{pH_{IW}})} + 10^{(\mathrm{pH_{EW}}-\mathrm{p}K\mathrm{aAcid})} + 10^{(\mathrm{pH_{IW}}-\mathrm{p}K\mathrm{aAcid})}]/\{2 + 10^{(\mathrm{p}K\mathrm{aBase}-\mathrm{pH_{EW}})} + 10^{(\mathrm{p}K\mathrm{aBase}-\mathrm{pH_{IW}})} + 10^{(\mathrm{pH_{EW}}-\mathrm{p}K\mathrm{aAcid})} + 10^{(\mathrm{pH_{IW}}-\mathrm{p}K\mathrm{aAcid})} + \frac{1-\mathrm{fu_{EW}}}{\mathrm{fu_{EW}}} + \mathrm{K}a \times [\mathrm{AP^-}] \times (10^{(\mathrm{p}K\mathrm{aBase}-\mathrm{pH_{IW}})} + 10^{(\mathrm{pH_{IW}}-\mathrm{p}K\mathrm{aAcid})}) + P \times V_{\mathrm{nlt}} + (0.3P + 0.7) \times V_{\mathrm{pht}}\} \quad (3.1)$$

For permeability-limited tissues (eq 3.2), the basic assumptions are as follows:

(a) the drug distribution throughout the tissue (between extracellular and intracellular compartments) is time-dependent;
(b) a difference in unbound, nonionized concentrations between intracellular and extracellular space can be maintained by active transport (influx or efflux). The intracellular concentration is determined by time-dependent transport processes (active influx, or passive diffusion). The intracellular fraction unbound can be calculated by modifying eq 3.1 to account only for intracellular processes:

$$\mathrm{fu_{IW}} = [1 + 10^{(\mathrm{p}K\mathrm{aBase}-\mathrm{pH_{IW}})} + 10^{(\mathrm{pH_{IW}}-\mathrm{p}K\mathrm{aAcid})}]/\{1 + 10^{(\mathrm{p}K\mathrm{aBase}-\mathrm{pH_{IW}})} + 10^{(\mathrm{pH_{IW}}-\mathrm{p}K\mathrm{aAcid})} + K\mathrm{a} \times [\mathrm{AP^-}] \times (10^{(\mathrm{p}K\mathrm{aBase}-\mathrm{pH_{IW}})} + 10^{(\mathrm{pH_{IW}}-\mathrm{p}K\mathrm{aAcid})}) + P \times V_{\mathrm{nlt}} + (0.3P + 0.7) \times V_{\mathrm{pht}}\} \quad (3.2)$$

For perfusion limited tissues, a partition coefficient, Kp, was used to calculate the amount of drug in the tissue at each time point. The partition coefficient was estimated from physicochemical properties (logD, $\mathrm{fu_P}$, and $\mathrm{fu_T}$) used as input into mechanistic tissue composition equations adapted from Rodgers and Rowland.[34,35] For this study, the two Rodgers and Rowland equations used for acids and for strong basis were combined into a single one. In this modified version of the equation (eq 3.3), developed by Lukacova et al., a continuous shift is allowed from neutrals and acids binding almost exclusively to albumin toward strong bases binding almost exclusively to acidic phospholipids.[41]

$$K\mathrm{pu} = V_{\mathrm{ew}} + \frac{1/X_{[\mathrm{D}],\mathrm{iw}}}{1/X_{[\mathrm{D}],\mathrm{p}}} V_{\mathrm{iw}} + \left(\frac{P \times V_{\mathrm{nlt}} + (0.3 \times P + 0.7) \times V_{\mathrm{pht}}}{1/X_{[\mathrm{D}],\mathrm{p}}}\right) + (\mathrm{Fn} + \mathrm{Fa}) \times \left[\frac{1}{\mathrm{fu_P}} - 1 - \left(\frac{P \times V_{\mathrm{nlp}} + (0.3 \times P + 0.7) \times V_{\mathrm{php}}}{1/X_{[\mathrm{D}],\mathrm{p}}}\right)\right] \times \mathrm{RAtp} + \mathrm{Fc} \times \left(\frac{K\mathrm{a} \times [\mathrm{AP}]_{\mathrm{T}}((1/X_{[\mathrm{D}],\mathrm{IW}}) - 1)}{1/X_{[\mathrm{D}],\mathrm{p}}}\right) \quad (3.3)$$

For the liver, considered as permeability-limited tissue, the calculation of extracellular $K\mathrm{p_{eL}}$ was based on the extracellular volume fraction of the tissue ($V_e = 0.159$ for the liver[38]), the hematocrit h (default = 0.45), the fraction unbound in plasma, $\mathrm{fu_p}$, and the fraction unbound in the tissue $\mathrm{fu_T}$ as described in Poulin and Theil (2000 and 2002):[38,42]

$$K\mathrm{p_{eL}} = \frac{V_e}{(1-h)} \times \frac{\mathrm{fu_P}}{\mathrm{fu_T}} \quad (3.4)$$

2. Perfusion-Limited Tissues. For a noneliminating perfusion-limited tissue the change in mass within the tissue was equal to the product of tissue blood flow (Q_T) and the difference between the blood concentrations in the arterial ($\mathrm{Cb_i}$) and venous compartments. Here, the venous blood concentration was represented as the ratio of tissue concen-

(41) Lukacova, V.; Parrott, N.; Lave, T.; Fraczkiewicz, G.; Bolger, M. B.; Woltosz, W. S. General Approach to Calculation of Tissue: Plasma Partition Coefficients for Physiologically Based Pharmacokinetic (PBPK) Modeling. AAPS Annual Meeting and Exposition, Atlanta 2008, Poster, November 16−20, 2008.
(42) Poulin, P.; Theil, F. P. A priori prediction of tissue:plasma partition coefficients of drugs to facilitate the use of physiologically-based pharmacokinetic models in drug discovery. *J. Pharm. Sci.* **2000**, *89*, 16–35.

tration (C_t) corrected for red blood cell binding (R_{bp}) divided by Kp.

$$V_t\frac{dC_t}{dt} = Q_T\left(Cb_i - \frac{C_t \times R_{bp}}{K\text{p}}\right) \quad (3.5)$$

To account for renal excretion, the mass balance equation for the kidney was modified from eq 3.5 as follows:

$$V_t\frac{dC_t}{dt} = Q_T\left(Cb_i - \frac{C_t \times R_{bp}}{K\text{p}}\right) - CL_{Rint,u}\left(\frac{C_t \times fu_P}{K\text{p}}\right) \quad (3.6)$$

where $CL_{Rint,u}$ is the unbound intrinsic clearance determined from observed *in vivo* plasmatic renal clearance (CL_{RP}). $CL_{Rint,u}$ was derived from the plasmatic renal clearance according to eq 3.7.[43]

$$CL_{Rint,u} = \frac{Q_T \times CL_{RP}}{fu_P(Q_T - CL_{RP}/R_{bp})} \quad (3.7)$$

3. Permeability-Limited Eliminating Tissue (Liver). The extracellular partition coefficient, $K\text{p}_{eL}$, was used to estimate the concentration of the drug in the extracellular compartment. The drug entry into the liver consisted of a passive permeability process parametrized as a permeability-surface area product (PS_{TC}) and of active uptake. Drug exit from the liver was driven by active efflux into bile. No active sinusoidal efflux back into the blood was considered. The active uptake parameters were determined *in vitro* and the active biliary excretion parameters were derived from *in vivo* experiments (Figure 2). As napsagatran and fexofenadine are metabolically stable compounds, no metabolic clearance was included in the model.

For the liver, considered as a permeability-limited tissue, the change in mass within the vascular and extracellular spaces was equal to the product of liver blood flow (Q_L) and the difference between the blood concentrations in the arterial (Cb_i) and venous compartments after subtraction of the active and passive permeabilities into the hepatocyte (eq 3.8). Here, the venous blood concentration was represented as the ratio of extracellular concentration (C_e) corrected for red blood cell binding (R_{bp}), divided by $K\text{p}_e$ and the passive and active transport, respectively, represented by PS_{TC}, J_{maxI} and $K_{mI,u}$ relative to the unbound concentrations in the extracellular ($C_{e,u}$) and tissue spaces ($C_{t,u}$).

$$\left(V_e + V_P\frac{R_{bp}}{K\text{p}_e}\right)\frac{dC_e}{dt} = Q_L\left(Cb_i - \frac{C_e R_{bp}}{K\text{p}_e}\right) - \left(\frac{J_{maxE} \times C_{e,u}}{K_{mI,u} + C_{e,u}} + PS_{TC}(C_{e,u} - C_{t,u})\right) \quad (3.8)$$

The liver blood flow in rat (Q_L) was taken as 60 mL/min/kg.

The mass balance equations for the intracellular space (eq 3.9) used in the model were as follows:

$$V_t\frac{dC_t}{dt} = \frac{J_{maxI} \times C_{e,u}}{K_{mI,u} + C_{e,u}} + PS_{TC}(C_{e,u} - C_{t,u}) - \left(\frac{J_{maxE} \times C_t \times fu_L}{C_t \times fu_L + K_{mE,u}} + PS_{TCAp} \times C_t \times fu_L\right) \quad (3.9)$$

Biliary excretion parameters J_{maxE}, $K_{mE,u}$ and PS_{TCAp} were derived from *in vivo* studies and eq 2.1. The basolateral uptake parameters derived from *in vitro* experiments using eq 1.1 (V_{maxI}, $K_{mI,u}$ and P_{dif}) were scaled to *in vivo* as described below. The affinity $K_{mI,u}$ estimated *in vitro* was assumed to be identical *in vivo*. PS_{TC} was reduced to a clearance term and scaled to *in vivo* according to eq 3.10:

$$PS_{TC} = P_{dif} \times \text{MTPMH} \times \text{HPGL} \times \text{liver weight} \times fu_{inc} \quad (3.10)$$

where MTPMH was the experimentally determined total protein content of hepatocytes (1.06 ± 0.18 mg/10^6 cells, $n = 5$), HPGL was the hepatocellularity (120×10^6 cells per g of liver[44]), and the liver weight was equal to 10.3 g.[45] The unbound fraction in the incubations, fu_{inc}, was considered to be 1 as no protein was added to the incubation medium.

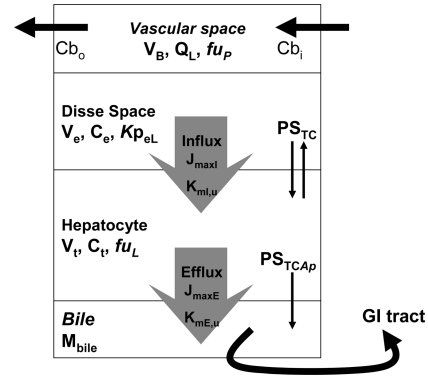

Figure 2. Liver compartment of the PBPK model. The vascular space is characterized by the liver blood flow (Q_L), a specific volume (V_B), drug concentration in (Cb_i) and out (Cb_o) the compartment and fraction unbound (fu_P); the drug entry in the space of Disse (volume V_e, drug concentration C_e) depends on extracellular coefficient of partition ($K\text{p}_{eL}$); the drug uptake in the intracellular compartment (volume V_t, drug concentration C_t, fraction unbound fu_L) depends on active (J_{maxI}, $K_{mI,u}$) and passive (PS_{TC}) transport processes and the drug export to the bile compartment depends on active (J_{maxE}, K_{mE}) and passive (PS_{TCAp}) efflux transport processes.

(43) Yang, J.; Jamei, M.; Yeo, K. R.; Rostami-Hodjegan, A.; Tucker, G. T. Misuse of the well-stirred model of hepatic drug clearance. *Drug Metab. Dispos.* **2007**, *35*, 501–2.

(44) Carlile, D. J.; Zomorodi, K.; Houston, J. B. Scaling factors to relate drug metabolic clearance in hepatic microsomes, isolated hepatocytes, and the intact liver: studies with induced livers involving diazepam. *Drug Metab. Dispos.* **1997**, *25*, 903–11.

(45) Houston, J. B. Utility of in vitro drug metabolism data in predicting in vivo metabolic clearance. *Biochem. Pharmacol.* **1994**, *47*, 1469–79.

Table 1. PBPK Input Data

	fexofenadine	napsagatran
Compounds' Physicochemical Properties		
biopharmaceutics classification BDDCS[9]	III[9]	III
mw	501.7	558.7
logD at pH 7.4	−0.01[a]	−0.4[a]
PAMPA Pe × 10^{-6} cm/s	4.49[a,16]	0[a]
pK_a	pK_a acid = 5.47[a]	pK_a acid = 3.7[a]
	pK_a base = 8.85[a]	pK_a base = 10.6[a]
solubility in phosphate buffer (mg/mL)	0.807[46]	0.744[a]
fu_p in rats	33.8%[47]	33.3%[a]
R_{bp}	0.895[a]	0.56[a]
Hepatic Transport Data		
Uptake from Plasma to Liver (*in Vitro* Data)		
$K_{ml,u}$		
(μM)	271 ± 35	88.4 ± 8.1
(mg/L eq. μg/mL)	136 ± 18	49.4 ± 4.5
V_{maxI} (pmol/mg/min)	3162 ± 274	384 ± 19
J_{maxI} (mg/s)	0.033 ± 0.003	0.0044 ± 0.0002
P_{dif} (μL/mg/min)	2.08 ± 0.67	0
PS_{TC} (mL/s)	0.045 ± 0.002	0
Excretion from Liver to Bile (*in Vivo* Data)		
$K_{mE,u}$ (μg/g eq. mg/L)	300[b]	0.53 ± 0.63
J_{maxE} (mg/s)	0.0054 ± 0.0006[b]	0.00036 ± 0.00009
PS_{TCAp} (mL/s)	0[b]	0
Observed Renal Clearances		
CL_{RP} calculated as fe × CL_P (mL/min/kg)	17.0 ± 1.7 (bolus 1 mg/kg)	14.6 ± 4.0 (bolus5 mg/kg)
	8.2 ± 11.1 (bolus 10 mg/kg)	20.2/4.1 (infusion 3.6 mg/kg)
	7.8 ± 2.5 (infusion 1 mg/kg)	24.3 ± 5.5 (infusion 30 mg/kg)
	4.8 ± 1.3 (infusion 10 mg/kg)	
	4.6 ± 2.7 (infusion 30 mg/kg)	

[a] Determined in house. [b] As no saturation was observed, a high $K_{mE,u}$ was fixed, and J_{maxE} and PS_{TCAp} fitted in consequence.

The same scaling factors were applied to V_{maxI}, where the molecular weight (mw) was used for the conversion to J_{maxI} (in mg/s).

$$J_{maxI} = V_{maxI} \times mw \times MTPMH \times HPGL \times \text{liver weight} \times fu_{inc} \quad (3.11)$$

4. Biliary Excretion and Enterohepatic Circulation. Equation 2.1 was used to model the excretion of nonmetabolized compound into bile, using the parameters fitted previously from *in vivo* profiles. As described in Figure 2, the amount of drug cleared through bile in rats continuously recirculates to the duodenum, where it is available for reabsorption.

5. Uncertainty Analysis. An uncertainty analysis was carried out to illustrate the impact of active and passive transport parameters on plasma, liver and bile profiles. All active transport parameters were changed by a factor of 10 (up and down) which was chosen arbitrarily to visualize the impact of the individual parameters. If equal to zero, the passive permeability was varied from 0 to a high but physiologically relevant value (highest value observed in rat hepatocytes according to Poirier et al. (2007) = 2.5 μL/mg/min[7]).

Results

Physicochemical Properties. The input parameters used for PBPK modeling of both fexofenadine and napsagatran are listed in Table 1. Both compounds are hydrophilic and zwitterionic with a strong basic and weak acidic pK_a. Both fexofenadine and napsagatran are BDDCS class III compounds characterized by a low permeability and good solubility. The blood/plasma ratio and plasma protein binding, also listed in Table 1, are similar for both compounds.

Hepatic Transport Data: Uptake (*in Vitro* Rat Hepatocytes) and Excretion (*in Vivo* Studies). The hepatic transport data are shown for both compounds in Table 1. Uptake parameters were obtained from *in vitro* hepatocyte

(46) Varma, M. V.; Panchagnula, R. Prediction of in vivo intestinal absorption enhancement on P-glycoprotein inhibition, from rat in situ permeability. *J. Pharm. Sci.* **2005**, *94*, 1694–704.

(47) Mahar Doan, K. M.; Wring, S. A.; Shampine, L. J.; Jordan, K. H.; Bishop, J. P.; Kratz, J.; Yang, E.; Serabjit-Singh, C. J.; Adkison, K. K.; Polli, J. W. Steady-state brain concentrations of antihistamines in rats: interplay of membrane permeability, P-glycoprotein efflux and plasma protein binding. *Pharmacology* **2004**, *72*, 92–8.

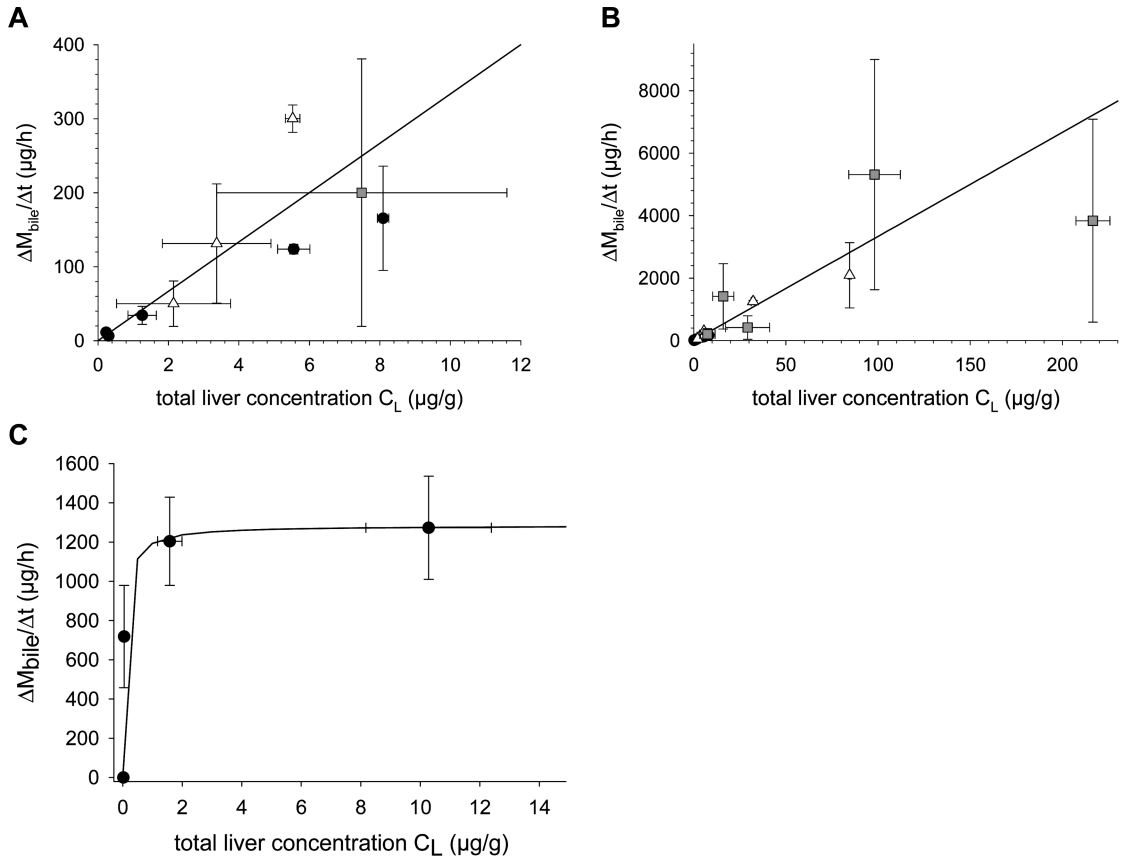

Figure 3. Observed biliary excretion rate profiles over total liver concentration. Equation 2.1 was used to calculate $K_{mE,u}$, J_{maxE} and PS_{TCAp} (fitted line on graph) values (cf. Table 1). A, B: Fexofenadine biliary excretion in bile-duct cannulated (BDC) rats dosed by iv infusion at 1 mg/kg (closed circles), 10 mg/kg (open triangles), 30 mg/kg (gray squares). A and B are on different scales. C: Napsagatran biliary excretion in BDC rats dosed by iv bolus at 5 mg/kg (closed circles).

incubations as described in Materials and Methods. Napsagatran showed a slightly higher affinity for liver uptake carriers (88 μM) compared to fexofenadine (271 μM). An 8-fold higher V_{maxI} was observed for fexofenadine (3162 pmol/mg/min) as compared to napsagatran (V_{maxI} 384 pmol/mg/min). The passive diffusion (P_{dif}) derived from the hepatocyte data was in accordance with previously determined passive permeabilities obtained with the PAMPA assay.[16] Thus, napsagatran showed no passive diffusion ($P_{dif} = 0$ and PAMPA Pe $= 0$) and fexofenadine exhibited a medium passive permeability ($P_{dif} = 2.08$ μL/mg/min and PAMPA Pe $= 4.49 \times 10^{-6}$ cm/s).

The excretion into bile was derived from *in vivo* biliary excretion and liver concentration data. The liver concentrations obtained for napsagatran after 5 mg/kg bolus administration are represented in Figure 3. The Michaelis−Menten parameters J_{maxE} and $K_{mE,u}$, and PS_{TCAp} for biliary excretion were obtained from these data. However the limited data and steep relationship between the napsagatran biliary excretion rate and liver concentration led to a high uncertainty in the estimation of $K_{mE,u}$, which was estimated to be below 3 μM. For fexofenadine, the biliary excretion rates increased linearly with liver concentrations (Figure 3) and no saturation of the biliary excretion rate was observed in the dose range investigated. Therefore, for further evaluation, $K_{mE,u}$ was arbitrarily set to a high value, ie 300 μg/g, and J_{maxE} and PS_{TCAp} were obtained by fitting the biliary excretion rates vs the liver concentration profiles. For fexofenadine, the excretion transport was found to be slower than the uptake: the intrinsic clearances calculated in nonsaturated conditions ($J_{max}/(K_{m,u} + C_u)$) were 285 μL/s and 17.8 μL/s for uptake and excretion, respectively, whereas for napsagatran the active uptake intrinsic clearance in a nonsaturated condition was lower than the excretion (88.9 μL/s for uptake and 679 μL/s for excretion). Thus fexofenadine tended to accumulate extensively in rat liver issue in contrast to napsagatran.

***In Vivo* Studies.** Table 2 lists the PK parameters derived from the plasma concentration time profiles. Bile-duct cannulated (BDC) rats and non-bile-duct cannulated rats, dosed with napsagatran at 5 mg/kg, showed identical plasma concentration vs time profiles; therefore the two groups were pooled together for further evaluations. Napsagatran plasma clearances and half-lives were comparable across doses.

In the case of fexofenadine, the BDC rats showed a different PK profile compared to non-bile-duct cannulated rats. The clearance appeared to be almost 2-fold lower in BDC rats compared to noncannulated rats. Therefore these data are presented separately.

Table 2. *In Vivo* Rat Study Design for Plasma PK Studies and Observed Parameters CL_P and $t_{1/2}$[a]

administration route	nominal dose (mg/kg)	number of rats	CL_P (mL/min/kg)	$t_{1/2}$ (h)
		Fexofenadine		
iv bolus	1	6	69.3 ± 5.4	0.91 ± 0.40
	10	3	52.8 ± 11.3	1.27 ± 0.02
30 min infusion	1	4	56.7 ± 5.6	0.55 ± 0.11
	10	4	33.3 ± 5.9	1.38 ± 0.36
	30	4	41.6 ± 15.4	1.24 ± 0.36
30 min infusion BDC[b]	1	2[c]	21.0/23.1*[d]	0.94/1.08
	10	3	21.0 ± 1.1*[d]	1.01 ± 0.25
	30	3	13.2 ± 1.2*[d]	1.25 ± 0.60
		Napsagatran		
iv bolus	5	5	59.0 ± 14.5	0.22 ± 0.06
90 min infusion	3.6	2	58.0/42.1	0.21/0.15
	30	2	77/102	0.24/0.24

[a] Mean values, or individual values if only 2 rats per group were used, are shown. [b] BDC = bile-duct cannulated rats. [c] One rat died 1 h after the start of the infusion in the 1 mg/kg BDC rat study, and values were excluded from the evaluation. [d] Statistically significant differences of the mean CL_P between noncannulated and BDC rats are shown by Student's *t* test: $*p < 0.05$.

PBPK Modeling. 1. Assumptions. The main assumptions used in building the PBPK model are summarized here. The distribution in the liver was treated as permeability limited. Bidirectional permeability was assumed at the apical membrane of the hepatocyte whereas unidirectional passive permeability was assumed for excretion from the hepatocyte into bile. No tissue permeability estimate was available for all the other tissues included in the PBPK model, i.e. kidney, heart, lung, adipose, bone marrows, brain, muscle, reproductive organs and skin. Therefore these tissues were treated as perfusion limited tissues. No enterohepatic recirculation was included into the model.

2. Input Data for PBPK−*K*p Values. The physicochemical properties together with the transport parameters for uptake and excretion and the renal clearances used for PBPK simulations are listed in Table 1. The fraction unbound in liver, fu_L, and the extracellular partition coefficients, Kp_{eL}, and *K*p values in other tissues were calculated as described in the methods and annexes and are available in Table 3. Both compounds showed similar binding parameters in liver, i.e. fu_L of 85.6% and 85.3%, respectively, for fexofenadine and napsagatran, and identical Kp_{eL} values of 0.11. Renal plasma clearances, CL_{RP}, were obtained from the *in vivo* data for input in PBPK modeling.

3. Uncertainty Analysis. The results from the uncertainty analysis are shown in Figure 4 for napsagatran and Figures 5, 6 and 7 for fexofenadine. The uptake parameters determined *in vitro* were key for the prediction of plasma exposure and biliary elimination, whereas the passive and active biliary excretion parameters had no influence on the napsagatran plasma and biliary excretion profiles. Excretion parameters are however important for the estimation of liver profiles. Similar findings were obtained for fexofenadine. Plasma and biliary excretion profiles were most sensitive to active uptake transport parameters, V_{maxI} and K_{mI}, while liver concentrations were very sensitive to both active and passive biliary excretion. For napsagatran, the observed liver concentrations needed to be corrected for blood and bile contents and this lead to a high uncertainty, as the calculated remaining bile amount in the collected liver accounted for most of the napsagatran quantity measured in the whole liver. For both compounds, active transport parameters had much more impact than passive permeability at both the basal and apical membranes.

Table 3. Major Calculated Data Input in PBPK: fu_L and Kp_{eL} for the Liver Compartment, *K*p for the Other Tissues

	fexofenadine	napsagatran
	Liver Tissue	
fu_L	85.6%	85.3%
Kp_{eL}	0.11	0.11
	Other Tissues	
*K*p		
lung	4.78	0.27
adipose	0.51	0.04
muscle	2.02	0.26
spleen	3.93	0.26
heart	2.86	0.26
brain	0.76	0.28
kidney	6.06	0.27
skin	1.76	0.22
reproductive organs	6.06	0.27
red marrow	0.93	0.15
yellow marrow	0.51	0.04
rest of body	3.93	0.26

4. Comparison Observed/Predicted (Profiles and Output Parameters). The predicted and observed major pharmacokinetic parameters for both napsagatran and fexofenadine are compared in Figure 8. After including a further empirical scaling factor of 10 for both compounds on the uptake clearance term, all parameters (CL_P, $t_{1/2}$, V_{dSS}, f_{bile}, C_{maxL}) were predicted within 2-fold and all profiles (plasma, liver and bile) were reasonably well predicted (Figures 4 to 7).

Discussion

Prediction of pharmacokinetic parameters from *in vitro* data remains an important challenge during drug discovery. The ability to predict human pharmacokinetics based on a combination of *in vitro* ADME properties and physicochemical properties integrated into physiologically based pharmacokinetic models has been demonstrated in a number of recent studies.[1−3] This approach proved to be very successful for lipophilic compounds mainly eliminated by liver metabolism and well permeable through cell membranes (BDDCS class 1 and 2 drugs). For such compounds a number of *in vitro* models such as liver microsomes or hepatocytes provide quantitative input parameters for metabolism and these models are widely used for compound selection during

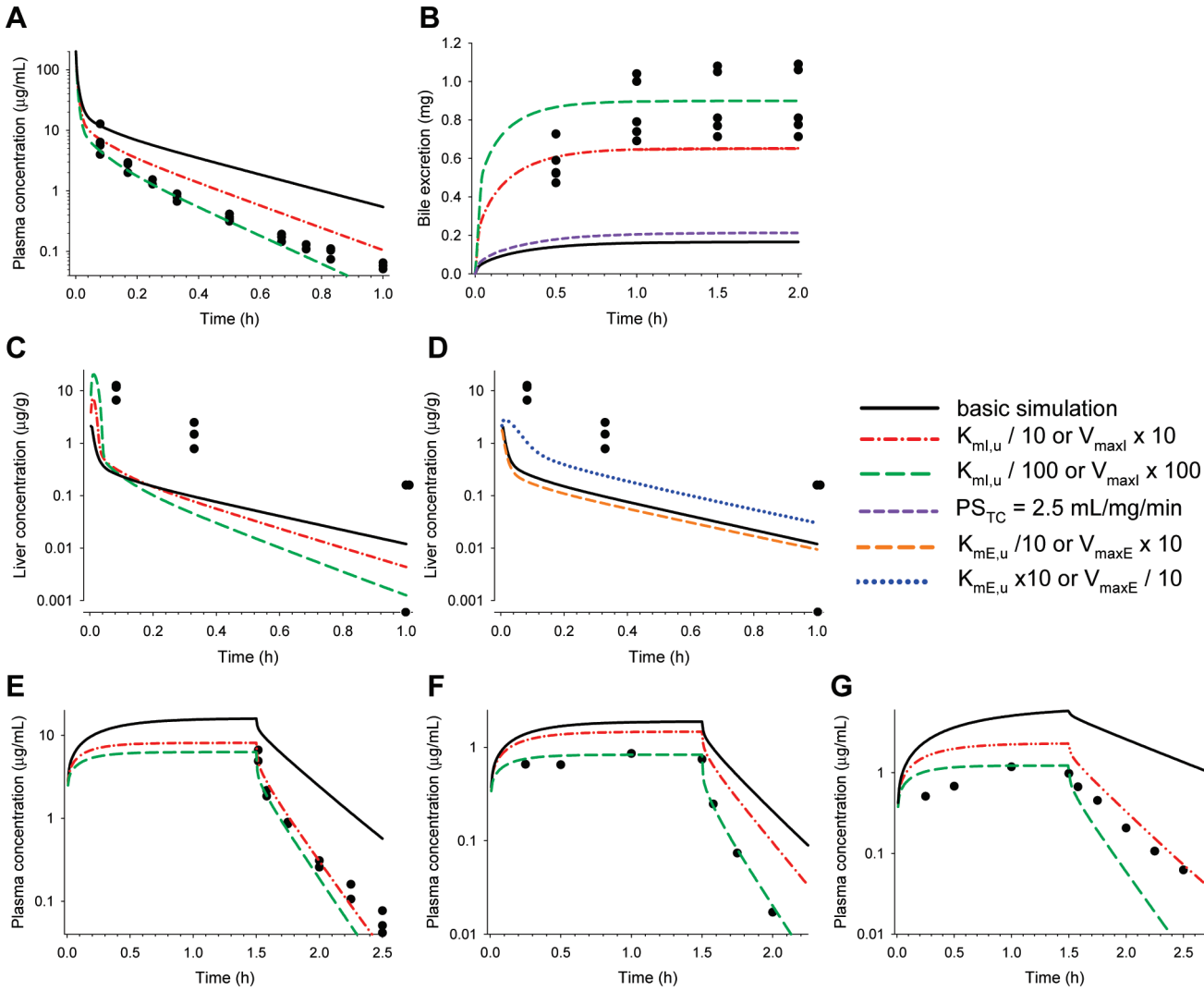

Figure 4. Uncertainty analysis on napsagatran profiles: impact of passive and active uptake (A−C, E−G) and excretion (D) transport parameters on plasma (A, E−G), bile (B) and liver (C, D) profiles; simulated (line) and observed (symbols) data are shown. Rats received an iv bolus of napsagatran 5 mg/kg (A−D) or a 90 min infusion at 30 mg/kg (E) or 3.6 mg/kg (F, G). Rats in F and G received the same dose but showed a different renal clearance. Excretion parameters had no impact on plasma and bile profiles, PS_{TC} had no impact on plasma and liver profiles, and PS_{TCAp} had no impact on any profile.

the drug discovery process and for quantitative predictions of *in vivo* clearance in animals and humans.[5−8] Such information proved also to be useful for quantitative prediction of full concentration versus time profiles in animals and human using physiologically based models.[1−3] Common approaches to optimize compounds during drug discovery are mainly based on solubility, lipophilicity, permeability and metabolic stability. The optimization of compound properties for improved metabolic stability and therefore reduced lipophilicity and permeability has contributed to shift the elimination routes toward non-metabolic processes.[10] As a consequence, transporter mediated processes are increasingly found to be responsible for clearance of compounds. Thus, besides hepatic metabolism it is increasingly recognized that uptake and efflux transport processes have a significant impact on hepatic clearance of new chemical entities.[48−50] Important limitations of the PBPK approach are realized for BDDCS class 3 and 4 compounds for which hepatic uptake and biliary elimination are likely to be major components of

(48) Evans, A. M. Membrane transport as a determinant of the hepatic elimination of drugs and metabolites. *Clin. Exp. Pharmacol. Physiol.* **1996**, *23*, 970–4.

(49) Yamazaki, M.; Suzuki, H.; Sugiyama, Y. Recent advances in carrier-mediated hepatic uptake and biliary excretion of xenobiotics. *Pharm. Res.* **1996**, *13*, 497–513.

(50) Kivisto, K. T.; Niemi, M. Influence of drug transporter polymorphisms on pravastatin pharmacokinetics in humans. *Pharm. Res.* **2007**, *24*, 239–47.

(51) Custodio, J. M.; Wu, C. Y.; Benet, L. Z. Predicting drug disposition, absorption/elimination/transporter interplay and the role of food on drug absorption. *Adv Drug Delivery Rev.* **2008**, *60*, 717–33.

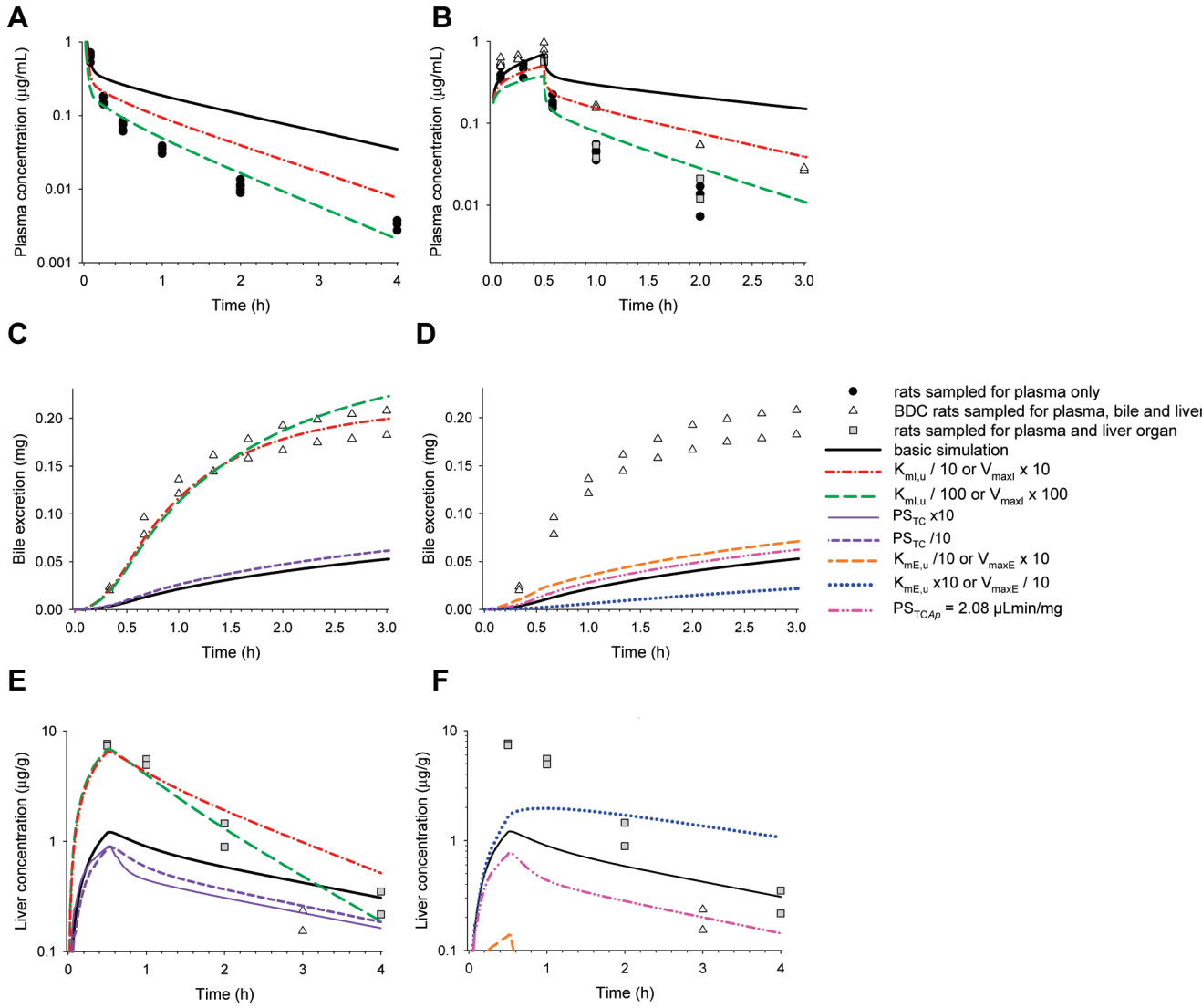

Figure 5. Uncertainty analysis on fexofenadine 1 mg/kg profiles: impact of passive and active uptake (A, B, C, E) and excretion (D, F) transport parameters on plasma (A, B), bile (C, D) and liver (E, F) profiles; simulated (line) and observed (symbols) data are shown. Rats received a 1 mg/kg fexofenadine iv bolus (A) or 30 min infusion (B−F). Excretion parameters and PS_{TC} had no impact on plasma profiles.

the elimination process.[9,51] For such compounds the assumptions of flow limited distribution and well mixed compartments are not valid and permeability limited distribution is apparent. Such processes can be addressed by the addition of permeability barriers for some tissues and by the incorporation of active uptake into liver, active efflux into bile, biliary elimination and enterohepatic recirculation. However, this improvement to current methodologies requires the availability of the appropriate quantitative input data as well as validation of the corresponding *in vitro* to *in vivo* scaling approaches.

In the process of building and testing such more complex, mechanistic liver models, two metabolically stable, BDCCS class III compounds were selected. Incorporation of transport processes was crucial for napsagatran and fexofenadine, which are metabolically stable; in the absence of any input parameter for liver elimination into the physiologically based pharmacokinetic model, the simulated plasma profile would only reflect the renal elimination and the plasma clearance would be underpredicted by more than 4-fold (data not shown). Thus, the mechanistic model to derive passive and active uptake parameters from hepatocytes as described in Poirier et al.[16] has been used in this study for napsagatran and fexofenadine. The resulting data were integrated into a physiologically based pharmacokinetic model together with *in vivo* biliary excretion data to simulate the full concentration time profiles in plasma, liver and bile. Since passive permeability reduces the impact of active transport processes on hepatic clearance, the compounds investigated in this study were chosen because they exhibited low passive permeability and their clearance was mainly driven by active transport processes. The data generated in this study in plated hepatocytes confirmed the low or nonsignificant contribution of passive permeability to hepatic clearance. The passive permeability of napsagatran was close to zero whereas the passive permeability for fexofenadine represented less than

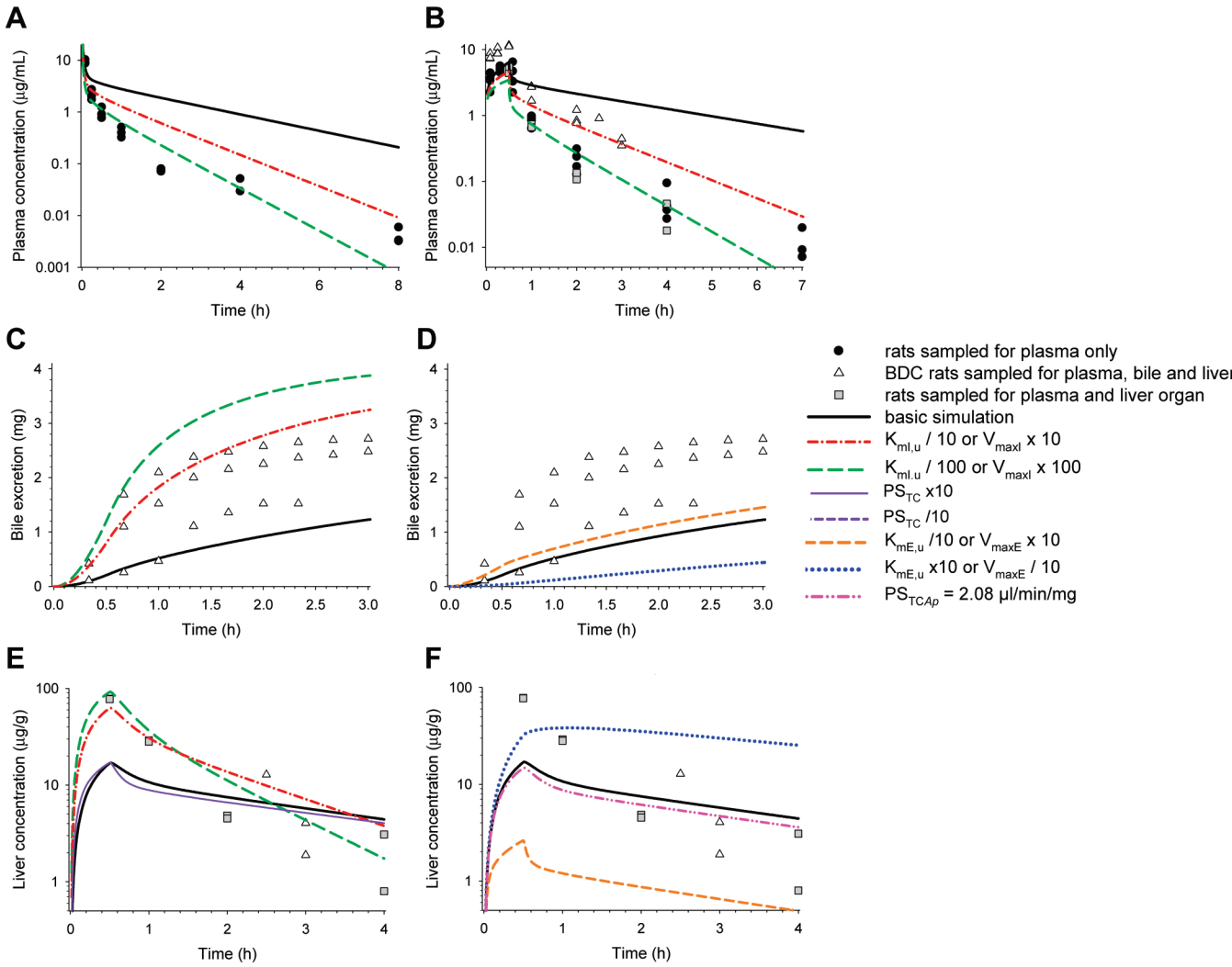

Figure 6. Uncertainty analysis on fexofenadine 10 mg/kg profiles: impact of passive and active uptake (A, B, C, E) and excretion (D, F) transport parameters on plasma (A, B), bile (C, D) and liver (E, F) profiles; simulated (line) and observed (symbols) data are shown. Rats received a 10 mg/kg fexofenadine iv bolus (A) or 30 min infusion (B to F). Excretion parameters had no impact on plasma profiles, PS_{TC} had not impact on plasma or bile profiles and PS_{TCAp} had no impact on bile profiles.

20% of the uptake clearance under linear conditions. Despite identical physicochemical properties, napsagatran and fexofenadine exhibited very different transport rates at the uptake and biliary excretion level. In contrast to napsagatran, which did not show any significant passive diffusion process, fexofenadine was transported into rat hepatocytes through both passive and active processes. For napsagatran the biliary excretion clearance (679 μL/s) tended to be faster than the uptake (89 μL/s), supporting the fact that very low liver concentrations were observed for this compound. In this case active uptake was the rate-limiting step for both plasma elimination and biliary excretion of napsagatran. The opposite was observed for fexofenadine: the uptake process (285 μL/s) was more efficient than the biliary excretion process (18 μL/s), which resulted in high liver concentrations for this compound.

The transport parameters, evaluated *in vitro* for uptake and *in vivo* for canalicular excretion, were used in a PBPK model including hepatic transport processes. In order to compare those predictions with observed profiles, *in vivo* studies were conducted for both compounds: plasma and liver sampling, and bile collection from BDC rats. Both compounds were mainly eliminated unchanged in bile as described previously.[22,25] The rat strain used for the napsagatran *in vivo* studies, originally performed in Lavé et al. (1999),[22] differed from the strain used for the preparation of the hepatocytes in this study. Ideally the same strain should have been used to build scaling factors. However, for fexofenadine the plasma profile and PK parameters in our study using Wistar rats dosed at 1 mg/kg bolus iv were in good accordance with results from Strelevitz et al. obtained in Sprague−Dawley rats.[52]

The plasma profiles observed for BDC rats dosed with fexofenadine appeared to differ from non bile-duct cannu-

(52) Strelevitz, T. J.; Foti, R. S.; Fisher, M. B. In vivo use of the P450 inactivator 1-aminobenzotriazole in the rat: varied dosing route to elucidate gut and liver contributions to first-pass and systemic clearance. *J. Pharm. Sci.* **2006**, *95*, 1334–41.

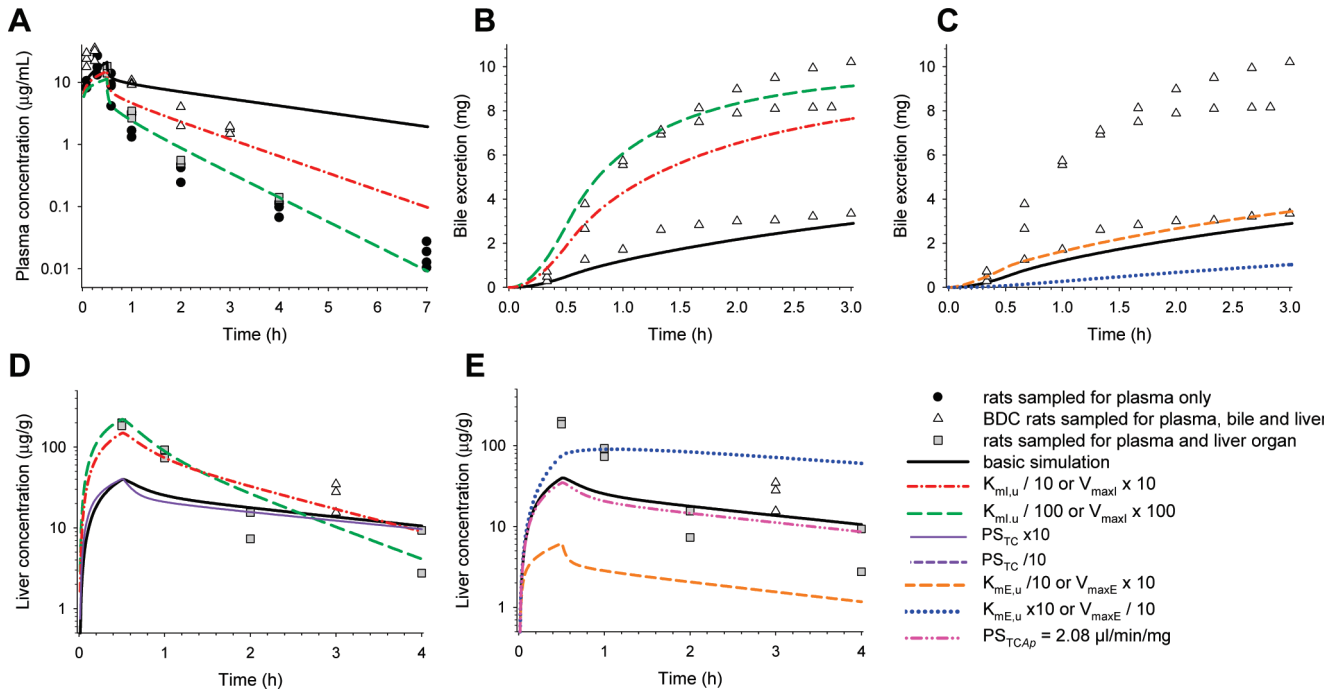

Figure 7. Uncertainty analysis on fexofenadine 30 mg/kg profiles: impact of passive and active uptake (A, B, D) and excretion (C, E) transport parameters on plasma (A), bile (B, C) and liver (D, E) profiles; simulated (line) and observed (symbols) data are shown. Rats received an iv infusion of fexofenadine 30 mg/kg. Excretion parameters had no impact on plasma profiles, PS_{TC} had no impact on plasma or bile profiles and PS_{TCAp} had no impact on bile profiles.

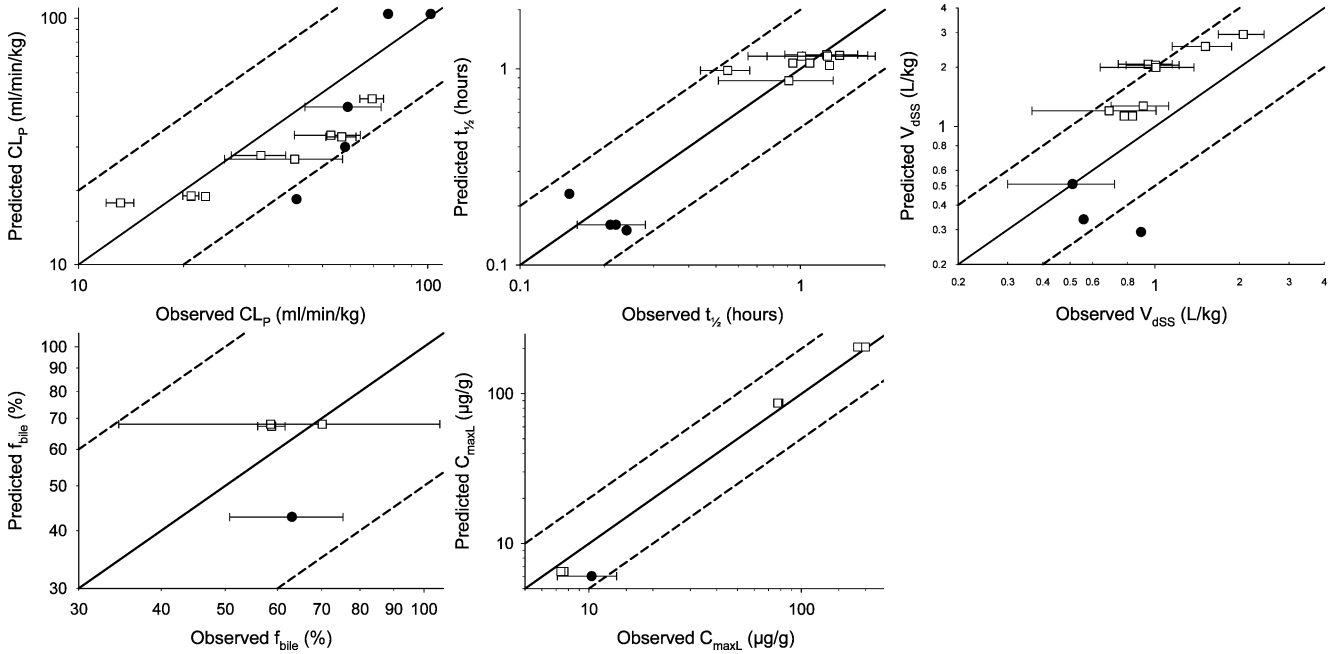

Figure 8. Predicted (using 10-fold correction factor on J_{maxl}) and observed kinetic parameters (CL_P, $t_{1/2}$, V_{dSS}, f_{bile}, C_{maxL}) for napsagatran (closed circles) and fexofenadine (open squares) at different doses, iv bolus and infusion. The black line is the line of identity, and the area between the dashed lines is the area with a less than 2-fold prediction error. In the case of only 2 rats per *in vivo* experimental group, individual values are shown.

lated rats. The increased plasma concentration might be related to an impairment of uptake capacity in BDC rats. In the case of fexofenadine, the BDC rats were bile-duct cannulated only one hour before the dosing and anesthetized during surgery and the study with blood and bile-sampling. The anesthetic used during the sampling (ketamine 0.12 μM and xylazine 0.018 μM) showed *in vitro* a strong inhibition of active fexofenadine uptake in hepatocytes

(data not shown), an interaction which could explain to some extent the decreased clearance and higher plasma profiles in the operated rats. For napsagatran, the BDC rats were cannulated multiple days in advance and were conscious during the experiment. This might explain why the plasma profiles were identical between the two groups for this compound.

An uncertainty analysis was performed in order to identify the most sensitive parameters which had to be optimized in order to match the *in vivo* profiles in the rat. As expected, uptake capacity was a very sensitive parameter for both plasma and biliary excretion profiles. An empirical factor of 10 had to be applied to the *in vitro* uptake clearance to match the *in vivo* plasma and liver concentrations and biliary excretion profiles. Interestingly the same factor was needed for both compounds. Although a scientific rationale for this difference is currently lacking for this limited data set, different possible explanations might include (i) reduced uptake activity in isolated hepatocytes *in vitro* compared to *in vivo* as it has already been suggested,[53,54] (ii) missing process(es) (intracellular binding, efflux back into medium) in the *in vitro* two-compartment model used for data analysis, (iii) misevaluation of the scaling factors (MTPMH, HPGL, cell volume) which were established for scaling of metabolic clearance, and (iv) bias in the incubation conditions and *in vitro* setting. Further work using more compounds is required to validate this approach and evaluate whether such empirical scaling factors apply across a range of compounds and transporters. A model incorporating *in vivo* and *in vitro* data from preclinical species to derive drug specific factors that would theoretically correct for any systematic difference between *in vitro* and *in vivo* parameters is currently under evaluation. Interestingly, similar adjustments were used in a recent publication for liver uptake[55] and are also used for metabolic stability where refinement and validation of the PBPK model in preclinical species as a first step is a common strategy to apply for predicting the human situation.[3,17,55−57]

As several drugs have already shown clinically significant drug interactions with fexofenadine linked to inhibition of liver uptake carriers,[23] the next step will be to apply the established PBPK models and *in vitro* transport and inhibition data involving the relevant transporters to understand the impact of such interactions on plasma, liver and bile profiles.

For both compounds, plasma, liver and bile concentration time profiles were reasonably well predicted based on *in vitro* transport parameters. The *in vivo* data did not exhibit significant nonlinearity as it might be expected when active transport processes are involved in elimination. However, the maximum plasma concentrations achieved by both napsagatran and fexofenadine were well below the K_{mI} calculated from *in vitro* hepatocyte data ($K_{mI} = K_{mI,u}/fu_p$), which were 148 μg/mL for napsagatran and 402 μg/mL for fexofenadine. For napsagatran, the observed plasma concentrations were always lower than 148 μg/mL and, in consequence, no saturation could be observed *in vivo*. The highest fexofenadine plasma concentration observed was around 30 μg/mL (30 mg/kg dose group), and no clear decrease of plasma clearance could be observed in the noncannulated rats. The model could therefore not be challenged for its ability to correctly predict nonlinear kinetics due to a saturation of active uptake processes.

The simulations of the different profiles in plasma, liver and bile were obtained on the basis of *in vitro* transport parameters for hepatic uptake. However, for hepatobiliary export, *in vivo* data had been used to derive biliary excretion transport clearance. While the prediction of liver concentrations would require *in vitro* estimates of the biliary excretion process, the uncertainty analysis clearly showed that the hepatic uptake parameters, based on scaled and adjusted *in vitro* transport data, were sufficient for the prediction of plasma profiles for the compounds studied here. In the case of napsagatran, where uptake was found to be rate-limiting, the uptake parameters were also key to estimate the biliary excretion profile. On the contrary, a reliable, quantitative assessment of the hepatobiliary export process is essential for the prediction of (free and total) liver concentrations. Currently this remains a challenge because of the (un)availability of predictive *in vitro* tools for the biliary excretion process. Furthermore, it is not easy to generate reliable *in vivo* (free and total) liver concentration data. When liver concentrations are low as a result of slow uptake and rapid biliary excretion, the contamination of the liver tissue with highly concentrated residual bile prevents a reliable determination of the drug concentration in liver tissue. Thus, in this study high uncertainty was associated with napsagatran liver concentrations. Such considerations are key when judging the accuracy of the simulation. This phenomenon was not observed in the case of fexofenadine for which the uptake process was faster than the biliary excretion process leading to accumulation in the liver. In this case the correction for residual bile and blood remaining in liver tissue had almost no impact on the observed liver concentrations.

Data derived from *in vivo* studies were used in this study to estimate apical export into bile, but several *in vitro* tools have been described to estimate this process. Double transfected cells or membrane vesicles expressing biliary

(53) Rippin, S. J.; Hagenbuch, B.; Meier, P. J.; Stieger, B. Cholestatic expression pattern of sinusoidal and canalicular organic anion transport systems in primary cultured rat hepatocytes. *Hepatology* **2001**, *33*, 776–82.

(54) Turncliff, R. Z.; Tian, X.; Brouwer, K. L. Effect of culture conditions on the expression and function of Bsep, Mrp2, and Mdr1a/b in sandwich-cultured rat hepatocytes. *Biochem. Pharmacol.* **2006**, *71*, 1520–9.

(55) Watanabe, T.; Kusuhara, H.; Maeda, K.; Shitara, Y.; Sugiyama, Y. Physiologically based pharmacokinetic modeling to predict transporter-mediated clearance and distribution of pravastatin in humans. *J. Pharmacol. Exp. Ther.* **2009**, *328*, 652–62.

(56) Lave, T.; Parrott, N.; Grimm, H. P.; Fleury, A.; Reddy, M. Challenges and opportunities with modelling and simulation in drug discovery and drug development. *Xenobiotica* **2007**, *37*, 1295–310.

(57) Naritomi, Y.; Terashita, S.; Kagayama, A.; Sugiyama, Y. Utility of hepatocytes in predicting drug metabolism: comparison of hepatic intrinsic clearance in rats and humans in vivo and in vitro. *Drug Metab. Dispos.* **2003**, *31*, 580–8.

export transporters can be useful to identify the involved transport protein, however the issue on how to scale such results to *in vivo* remains.[1,58] Recently the expression levels of 34 transport proteins in liver and other organs of mouse were determined using LC/MS/MS by Kamiie et al.[59] This approach brings very useful information for the *in vitro* to *in vivo* extrapolation of active transport data; however a similar picture for rat and mainly human tissues is currently still missing. Rat hepatocytes in sandwich culture have been used to calculate *in vitro* biliary clearances characterizing in a single tool basolateral uptake and canalicular excretion.[60−63] Whereas the rank order of overall biliary clearances was consistent from *in vitro* to *in vivo*,[62] this method does not allow isolation of the apical transport process nor the calculation of corresponding Michaelis−Menten parameters necessary for the parametrization of the biliary excretion in a PBPK model. For a drug similar to napsagatran, showing a slow uptake and fast canalicular export, the determination of the rate-limiting step can be assessed in primary hepatocytes. For a drug with properties similar to fexofenadine, showing a fast uptake and slow canalicular export, the rate-limiting step for plasma exposure remains uptake transport. And with such properties, canalicular excretion might be difficult to assess experimentally in hepatocytes in sandwich culture due to the very low amount of drug excreted into the bile pockets relative to the high amount of drug remaining within the cells. Further development in the area of predictive experimental tools seems to be necessary to close this gap and allow quantitative measurements of hepatic export rates.

One additional issue in estimating the liver concentration is the evaluation of the free compound concentration. Active uptake typically leads to an increase in unbound concentration within the hepatocyte relative to the extracellular concentration. Both compounds studied here are hydrophilic and exhibit low cellular binding (calculated $fu_L \sim 85\%$ for both compounds); it can therefore be reasonably assumed that most of the intracellular compound is unbound and therefore available for the canalicular excretory systems. Paine et al.[17] proposed to express the *in vitro* clearance from the medium in terms of passive, uptake, efflux, and metabolic intrinsic clearances as previously described by Shitara et al. (2005) and Webborn et al. (2007).[64,65] Derived from this equation Paine et al. calculated a ratio (Ψ) of the free concentration inside the cell relative to the free concentration in the medium depending on intrinsic clearances of sinusoidal uptake (active and passive), sinusoidal efflux and metabolism (eq 9[17]). This ratio is an interesting parameter in drug development as it could give insight into the free liver concentration. If this equation was applied to our experimental *in vitro* data of fexofenadine, without considering metabolism nor sinusoidal efflux, Ψ was reduced to the ratio of the added passive and active uptake clearances under linear conditions ($P_{dif} + V_{maxI}/K_{mI,u}$) over the passive clearance alone (P_{dif}). We obtained a ratio $\Psi = 6.6$. This ratio was compared to the ratio estimated from our PBPK model used to simulate liver and plasma free concentrations but excluding biliary excretion. At steady state the ratio of free concentrations was around 7.4, hence similar to the one obtained *in vitro* using Paine's equation. Including biliary excretion in the PBPK simulation this ratio was reduced to 1.6 obviously as a result of the excretion of unchanged compound into bile (which is not parametrized in Paine's equation).

In conclusion, the plasma profiles of napsagatran and fexofenadine, which are both mainly eliminated by active transport processes, could be simulated based on data from *in vitro* hepatic uptake experiments. The hepatic elimination of compounds with similar properties (BDDCS class 3 and 4 compounds) could thus be similarly predicted based on refined *in vitro* uptake data using primary hepatocytes. However, the prediction of liver concentrations, total and free, remains challenging in the absence of fully validated quantitative *in vitro* tools for biliary export processes. Further work using more compounds is required to validate this approach and to evaluate whether empirical scaling factors, found to be needed for uptake, apply across a range of compounds and transporters involved.

Abbreviations Used

fu_p	fraction unbound in plasma
HPGL	hepatocytes per gram of liver
$K_{m,u}$	Michaelis−Menten affinity constant unbound (I influx, E efflux)
MTPMH	mg of total protein per million hepatocytes

(58) Kitamura, S.; Maeda, K.; Sugiyama, Y. Recent progresses in the experimental methods and evaluation strategies of transporter functions for the prediction of the pharmacokinetics in humans. *Naunyn-Schmiedebergs Arch. Pharmacol.* **2008**, *377*, 617–28.

(59) Kamiie, J.; Ohtsuki, S.; Iwase, R.; Ohmine, K.; Katsukura, Y.; Yanai, K.; Sekine, Y.; Uchida, Y.; Ito, S.; Terasaki, T. Quantitative atlas of membrane transporter proteins: development and application of a highly sensitive simultaneous LC/MS/MS method combined with novel in-silico peptide selection criteria. *Pharm. Res.* **2008**, *25*, 1469–83.

(60) Liu, X.; Chism, J. P.; LeCluyse, E. L.; Brouwer, K. R.; Brouwer, K. L. Correlation of biliary excretion in sandwich-cultured rat hepatocytes and in vivo in rats. *Drug Metab. Dispos.* **1999**, *27*, 637–44.

(61) Ghibellini, G.; Vasist, L. S.; Leslie, E. M.; Heizer, W. D.; Kowalsky, R. J.; Calvo, B. F.; Brouwer, K. L. In vitro-in vivo correlation of hepatobiliary drug clearance in humans. *Clin. Pharmacol. Ther.* **2007**, *81*, 406–13.

(62) Abe, K.; Bridges, A. S.; Yue, W.; Brouwer, K. L. In vitro biliary clearance of angiotensin II receptor blockers and 3-hydroxy-3-methylglutaryl-coenzyme A reductase inhibitors in sandwich-cultured rat hepatocytes: comparison with in vivo biliary clearance. *J. Pharmacol. Exp. Ther.* **2008**, *326*, 983–90.

(63) Fukuda, H.; Ohashi, R.; Tsuda-Tsukimoto, M.; Tamai, I. Effect of plasma protein binding on in vitro-in vivo correlation of biliary excretion of drugs evaluated by sandwich-cultured rat hepatocytes. *Drug Metab. Dispos.* **2008**, *36*, 1275–82.

(64) Webborn, P. J.; Parker, A. J.; Denton, R. L.; Riley, R. J. In vitro-in vivo extrapolation of hepatic clearance involving active uptake: Theoretical and experimental aspects. *Xenobiotica* **2007**, *37*, 1090–109.

(65) Shitara, Y.; Sato, H.; Sugiyama, Y. Evaluation of drug-drug interaction in the hepatobiliary and renal transport of drugs. *Annu. Rev. Pharmacol. Toxicol.* **2005**, *45*, 689–723.

mw	molecular weight
PBPK	physiologically based pharmacokinetic
P_{dif}	passive diffusion at the basolateral membrane determined *in vitro*
R_{bp}	blood−plasma ratio
V_{max}	Michaelis−Menten maximum velocity (I influx, E efflux)

In Vitro: Mechanistic Model

A_{int}	quantity of compound in one well
C_{int}	compound concentration in intracellular space *in vitro*
C_{ex}	compound concentration in the medium *in vitro*
f_b	fraction nonspecifically bound in the *in vitro* system
U_{int}	total quantity of protein per well
V_{int}	intracellular volume of all cells in one well
V_{ex}	volume of the incubation medium *in vitro*

In Vivo: Pharmacokinetic Analysis

AUC	area under the concentration time curve
AUMC	area under the moment curve
β	slope of the terminal phase
BDC	bile duct cannulated rats
C_L	total concentration in liver *in vivo*
C_{maxL}	maximum concentration in liver *in vivo*
C_P	total concentration in plasma *in vivo*
CL_{Bile}	biliary clearance (excretion from plasma to bile)
CL_{Blood}	total blood clearance
CL_E	excretion clearance (excretion from liver to bile)
CL_P	plasma clearance
f_{bile}	fraction of the dose excreted unchanged in bile
fe	fraction of the dose excreted unchanged in urine
$t_{1/2}$	half-life
τ	infusion time

Whole PBPK Model

Cb	total concentration in blood *in vivo*
Cb_i, Cb_o	blood concentration in (arterial) and out (venous) of tissue
C_e	drug concentration in extracellular space (u = unbound) *in vivo*
C_t	drug concentration in intracellular space (u = unbound) *in vivo*
$CL_{int,u}$	intrinsic clearance unbound
CL_{RP}	plasma renal clearance $CL_{RP} = CL_P \times fe$
fu_{inc}	fraction unbound in the *in vitro* incubation
fu_L	fraction unbound in liver
fu_T	fraction unbound in tissue
h	hematocrit
J_{max}	Michaelis−Menten maximum velocity scaled to *in vivo* (I influx, E efflux)
Kp	partition coefficient
$K p_{eL}$	partition coefficient in extracellular space in liver (= in Disse space)
M_b	amount of drug cleared by biliary excretion
PS_{TC}	permeability−surface area product at the basolateral membrane
PS_{TCAp}	permeability−surface area product at the apical membrane
Q_T	tissue blood flow
Q_L	liver blood flow
V_e	extracellular volume fraction of liver tissue
V_B	blood volume
V_t	tissue volume

*K*p and fu_T Calculations

$[AP^-]$	concentration of acidic phospholipids (extracted from ref 41)
Fc	fraction of drug with positive charge in plasma
(Fn + Fa)	fraction of drug without positive charge in plasma
fu_{EW}	extracellular unbound fraction
fu_{IW}	intracellular unbound fraction
fu_p	fraction unbound in plasma
fu_T	fraction unbound in tissue
Ka	association constant with acidic phospholipids
Kpu	unbound tissue:plasma partition coefficient
P	*n*-octanol:water partition coefficient
pH_{EW}	pH of extracellular tissue water
pH_{IW}	pH of intracellular tissue water
RAtp	the ratio of albumin (for nonionizable compounds) or lipoprotein (for ionizable compounds) concentration found in tissue over plasma
V_{nlt}, V_{pht}, V_{ew}, V_{iw}	volume fraction of neutral lipids, phospholipids, intracellular and extracellular water in tissues
V_{nlp}, V_{php}	volume fraction of neutral lipids and phospholipids in plasma
$X_{[D],IW}$, $X_{[D],P}$	fraction of neutral drug species in intracellular space (pH = 7) and plasma (pH = 7.4)

Acknowledgment. The authors thank Philippe Coassolo for advice and support in many helpful discussions throughout this project, Véronique Dall'Asen and Marie-Stella Gruyer for performing the *in vivo* studies and Isabelle Walter for technical support in sample analysis.

MP8002495